Chapter 7
Metal Enzymes in "Impossible" Microorganisms Catalyzing the Anaerobic Oxidation of Ammonium and Methane

Joachim Reimann, Mike S.M. Jetten, and Jan T. Keltjens

Contents

J. Reimann • M.S.M. Jetten (✉) • J.T. Keltjens (✉)
Department of Microbiology, Institute of Wetland and Water Research (IWWR), Radboud University of Nijmegen, Heyendaalseweg 135, 6525AJ Nijmegen, The Netherlands
e-mail: j.reimann@science.ru.nl; m.jetten@science.ru.nl; j.keltjens@science.ru.nl

P.M.H. Kroneck, M.E. Sosa Torres (eds.), *Sustaining Life on Planet Earth: Metalloenzymes Mastering Dioxygen and Other Chewy Gases*, Metal Ions in Life Sciences 15, DOI 10.1007/978-3-319-12415-5_7

Abstract Ammonium and methane are inert molecules and dedicated enzymes are required to break up the N-H and C-H bonds. Until recently, only aerobic microorganisms were known to grow by the oxidation of ammonium or methane. Apart from respiration, oxygen was specifically utilized to activate the inert substrates. The presumed obligatory need for oxygen may have resisted the search for microorganisms that are capable of the anaerobic oxidation of ammonium and of methane. However extremely slowly growing, these "impossible" organisms exist and they found other means to tackle ammonium and methane. Anaerobic ammonium-oxidizing (anammox) bacteria use the oxidative power of nitric oxide (NO) by forging this molecule to ammonium, thereby making hydrazine (N_2H_4). Nitrite-dependent anaerobic methane oxidizers (N-DAMO) again take advantage of NO, but now apparently disproportionating the compound into dinitrogen and dioxygen gas. This intracellularly produced dioxygen enables N-DAMO bacteria to adopt an aerobic mechanism for methane oxidation.

Although our understanding is only emerging how hydrazine synthase and the NO dismutase act, it seems clear that reactions fully rely on metal-based catalyses known from other enzymes. Metal-dependent conversions not only hold for these key enzymes, but for most other reactions in the central catabolic pathways, again supported by well-studied enzymes from model organisms, but adapted to own specific needs. Remarkably, those accessory catabolic enzymes are not unique for anammox bacteria and N-DAMO. Close homologs are found in protein databases where those homologs derive from (partly) known, but in most cases unknown species that together comprise an only poorly comprehended microbial world.

Keywords anaerobic methane oxidation • anammox • denitrification • hydrazine oxidation • hydrazine synthesis • methanol dehydrogenase • nitric oxide • octaheme proteins

Please cite as: *Met. Ions Life Sci.* 15 (2015) 257–313

1 Introduction

Ammonia and methane are rather inert molecules, which is due to the high bond dissociation energy of the N-H (~400 $kJ \cdot mole^{-1}$) and C-H (429 $kJ \cdot mole^{-1}$) bonds. Aerobic ammonium-oxidizing and methane-oxidizing microorganisms are able to break up these bonds using the oxidative power of oxygen. By the action of two evolutionary highly related membrane-bound iron/copper enzymes, ammonia monooxygenase (AMO) and particulate methane monooxygenase (pMMO), ammonia and methane are activated to more accessible hydroxylamine (NH_2OH) and methanol (CH_3OH), respectively [1–3]. Besides pMMO, aerobic methane-oxidizing bacteria, the methanotrophs, can dispose of the unrelated soluble iron-only methane monooxygenase (sMMO) for methane activation (see Chapter 6 of this volume). Aerobic ammonium-oxidizing bacteria (AOB) and aerobic methanotrophs have been investigated for more than a century. All species studied until lately were members of the domain of Bacteria, but also ammonium-oxidizing Archaea (AOA) are known by now [4]. Although AOA typically thrive at very low oxygen concentrations, they too depend on oxygen to convert ammonium into hydroxylamine [5, 6].

The common notion that oxygen would be indispensable for ammonium and methane conversion may have blindfolded the search for microorganisms that would make a living of the oxidation of these substrates with electron acceptors other than O_2. Today we know that these "impossible" microorganisms do exist and in this chapter we will go into the biochemical basis of two groups of bacteria that drive ammonium and methane conversion with nitrite as the oxidant: The anaerobic ammonium-oxidizing (anammox) bacteria and the nitrite/nitrate-dependent anaerobic methane oxidizers (N-DAMO). Characteristics of these organisms are extreme slow growth rates, and the requirement of dedicated enrichment techniques and molecular detection tools [7, 8], factors that may have impeded an earlier identification.

Anammox bacteria have been first described only 20 years ago [9]. The active search for these organisms was spurred by the observation that ammonium disappeared in laboratory wastewater treatment reactors in the apparent absence of O_2 and as the result of a biological agent [9]. Following their first enrichment [10], anammox bacteria have been detected in a multitude of species and subspecies by now [11, 12]. They have been found worldwide and occur in essentially each anaerobic environment where fixed nitrogen (ammonium, nitrate, nitrite) is lost as dinitrogen gas (N_2). In many of these ecosystems, anammox bacteria play a key role in nitrogen cycle processes. Apart from their biogeochemical relevance, anammox bacteria offer us an economically attractive and environmentally friendly alternative to current wastewater treatment technology [13].

Anaerobic oxidation of methane is performed by two completely different groups of microorganisms: Archaea and members of the NC10 phylum of Bacteria. Archaeal methane oxidizers are found in deep-sea methane seeps where they couple, either or not in symbiotic interaction, methane oxidation with the reduction of sulfate [14]. Next to this, an archaeal enrichment culture designated *Candidatus* 'Methanoperedens nitroreducens' was recently described that was able of methane

oxidation at the expense of nitrate [15]. Intriguingly, the process took place in concurrence with anammox bacteria. Even so intriguingly, the original NC10 enrichment culture grown on methane and nitrate harbored a significant population of Archaea that phylogenetically affiliated those of the sulfate- and nitrate-reducing systems [16]. The archaeal species disappeared completely when the NC10 culture was shifted from nitrate to nitrite [17]. Although many details still have to be resolved, it seems clear that methane oxidation by Archaea is achieved by the reversal of the methane formation pathway [14], which is described in Chapter 6 of Vol. 14 of this series [138]. NC10 bacteria, represented by *Candidatus* 'Methanomirabilis oxyfera' [18], employ another strategy to tackle methane. These bacteria produce oxygen themselves, allowing the monooxygenation of methane into methanol that is subsequently oxidized to CO_2, as is carried out by aerobic methanotrophs [19].

Considering the inert nature of ammonium and methane, the primary question was how both substrates are activated by anammox and N-DAMO bacteria with nitrite (or nitrate) as oxidant. Whereas we are only at the beginning of a fundamental understanding of the molecular mechanisms underlying the anammox and N-DAMO processes, it has become clear that these microorganisms evolved novel biochemical systems to catalyze these reactions. This biochemistry is fully metal ion-based. However, not only the specific activation reactions are supported by metal chemistry. Most of the other pathway key reactions rely, in some way or another, on metal ions (Figure 1 in Section 2.1 and Figure 2 in Section 2.2). Here, anammox and N-DAMO bacteria take advantage of enzyme systems already known from other organisms, which have been adapted to own metabolic requirements by subtle structural modifications.

2 Pathways of Nitrite-Driven Anaerobic Oxidation of Ammonium and Methane

Anammox bacteria are autotrophic microorganisms, i.e., they are able to use CO_2 as the sole carbon source [10]. The energy for growth is obtained from the oxidation of ammonium with nitrite at which N_2 is produced as the end product (eq. 1). Principally, also ammonium oxidation coupled to nitrate reduction would provide sufficient energy to sustain growth (eq. 2), but this process does not comply with the biochemistry as far as we know it and highly enriched laboratory cultures are obtained only with nitrite.

$$NH_4^+ + NO_2^- \rightarrow N_2 + 2\,H_2O \qquad \left(\Delta G^{0\prime} = -357\,\mathrm{kJ}\cdot\mathrm{mol}^{-1}N_2\right) \quad (1)$$

$$5\,NH_4^+ + 3\,NO_3^- \rightarrow 4\,N_2 + 9\,H_2O + 2\,H^+ \qquad \left(\Delta G^{0\prime} = -452\,\mathrm{kJ}\cdot\mathrm{mol}^{-1}N_2\right) \quad (2)$$

$$3\ CH_4 + 8\ NO_2^- + 8\ H^+ \rightarrow 3\ CO_2 + 4\ N_2 + 10\ H_2O$$

$$\left(\Delta G^{0\prime} = -696\,\text{kJ} \cdot \text{mol}^{-1}N_2\right) \quad (3)$$

$$5\ CH_4 + 8\ NO_3^- + 8\ H^+ \rightarrow 5\ CO_2 + 4\ N_2 + 14\ H_2O$$

$$\left(\Delta G^{0\prime} = -613\,\text{kJ} \cdot \text{mol}^{-1}N_2\right) \quad (4)$$

Like anammox bacteria, *M. oxyfera* is an autotroph. With methane as electron donor, nitrite is reduced in catabolism to N_2, as in anammox bacteria (eq. 3). Theoretically, nitrate might act as an electron acceptor (eq. 4), but its use resists a proper redox balance (see Section 2.2). In laboratory practice, enrichment of *M. oxyfera* is only achieved with nitrite [17, 18].

Before discussing the individual biochemical reactions, we will first give an overview of how these steps are connected in the central catabolic pathways of the anammox and N-DAMO bacteria.

2.1 The Anammox Pathway

The crucial question at the start of anammox biochemistry was how ammonium could be activated in the apparent absence of oxygen. The clue to its understanding came from the fortuitous observation that metabolism by whole cells of ammonium and hydroxylamine, an artificial substrate, was accompanied by the transient accumulation of hydrazine (N_2H_4) [20]. Subsequent whole cell and biochemical studies established the role of hydrazine as an intermediate, also under physiological conditions [21, 22]. These studies identified a second intermediate proposed earlier, NO [21], while their results disfavored a role as such of hydroxylamine, as postulated initially [20]. Our current understanding is that anammox catabolism essentially is comprised of three consecutive reactions with two intermediates: (1) the one-electron reduction of nitrite to NO catalyzed by a nitrite reductase (Nir), (2) the condensation of ammonium and NO together with the input of three electrons leading to hydrazine, and (3) the oxidation of hydrazine to N_2, which generates four electrons that drive steps (1) and (2) in a cyclic way (Figure 1).

In this scheme (Figure 1), hydrazine synthesis would be catalyzed by a biochemical novelty, hydrazine synthase (HZS) [21]. Hydrazine oxidation would be brought about by hydrazine dehydrogenase/oxidase (HDH/HZO) representing a specific variant of the octaheme hydroxylamine oxidoreductase (HAO), a key enzyme in AOB (see Section 3.3.1). These expectations have been confirmed by the isolation and (initial) characterization of anammox enzymes [22]. Anammox metabolism as depicted in Figure 1 proceeds with a cyclic electron flow. This cyclic flow would take place such that oxidation and reduction reactions performed by membrane-bound

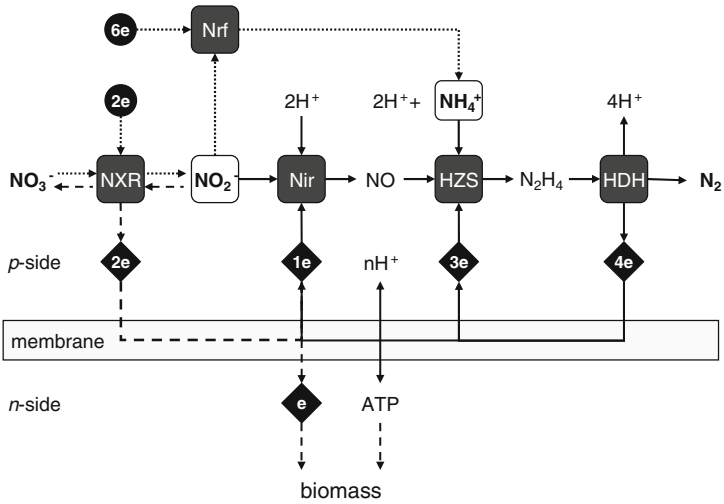

Figure 1 Scheme of the anaerobic ammonium oxidation (anammox) process with nitric oxide (NO) and hydrazine (N_2H_4) as intermediates and dinitrogen (N_2) as the end product. Primary substrates, ammonium (NH_4^+) and nitrite (NO_2^-), are indicated by the rounded squares. Reactions catalyzed by metal-ion-dependent enzymes are highlighted by dark grey rounded squares. Electron transfer processes within the cell are represented by black diamonds. Proton-motive force-driven ATP synthesis is schematically shown by proton translocation towards the positive (*p*-) side of the membrane system and ATP generation at the negative (*n*-) side. The *p*- and *n*-sides are the anammoxosome intracellular organelle and the cell cytoplasm, respectively. Electrons used for biosynthetic reduction reactions are replenished to the anammox cyclic electron flow by the oxidation of nitrite (dashed lines). "Disguised denitrification" by the reduction of nitrate or nitrite to ammonium at the expense of external organic or inorganic electron donors (black circles) is indicated by dotted lines. Abbreviations: HDH, hydrazine dehydrogenase; HZS, hydrazine synthase; Nir, nitrite reductase; Nrf, ammonium-forming nitrite reductase; NXR, nitrite:nitrate oxidoreductase.

processes are connected with the pumping of protons across these membranes, thus sustaining a proton-motive force to drive ATP synthesis. In anammox bacteria, respiratory processes would reside at a large intracellular cell organelle, termed the anammoxosome [23]. Present evidence supports such chemiosmotic mechanism in all major respects. Moreover, ongoing research underpins the central role of the anammoxosome in energy metabolism [24]. However, the detailed discussion of anammox energy metabolism is out of scope of the present chapter and we would like to refer interested readers to recent reviews that have been published on this matter [25, 26].

Reductive catabolic reactions in CO_2 fixation draw from the cyclic electron flow and electrons have to be replenished. The longstanding observation that autotrophic growth of anammox bacteria is always associated with the oxidation of nitrite to nitrate indicates that the electrons derive from nitrite [7]. The question how these electrons enter the cycle has not been resolved, considering that nitrite

is a relative poor electron donor (E_0' $NO_3^-/NO_2^- = +0.43$ V). Nevertheless, anammox cells contain high amounts of the iron-molybdoprotein nitrite:nitrate oxidoreductase (NXR), which is related to nitrate reductase found in denitrifiers (see Section 3.4.1). Indeed, NXR is capable of nitrate reduction [27] implying that anammox bacteria also use nitrate as terminal electron acceptor (eq. 2). Under chemolithoautotrophic conditions, i.e., with ammonium as the only electron donor, this is impossible. The reason for this is that in order to be reduced to nitrite, nitrate reduction needs electrons that drain the cyclic electron flow without replenishment. However, when grown in the presence of one of many different external inorganic or organic electron donors nitrate can be reduced to nitrite to support the anammox process (Figure 1) [28]. Under such conditions anammox bacteria may present themselves "disguised" as denitrifiers [28]. Now, half of the nitrite formed from nitrate is reduced to ammonia, which combines with the other half of nitrite in the anammox process. The apparent result is the complete reduction of nitrate into N_2, as is done by true denitrifiers. The reduction of nitrite into ammonia requires an ammonium-forming nitrite reductase as described in Chapter 9 of ref. [138]. The nature of this nitrite reductase in anammox bacteria will be the topic of Section 3.4.2.

2.2 *The Pathway of Nitrite-Driven Methane Oxidation*

An answer how *M. oxyfera* could couple the anaerobic oxidation of methane with the reduction to nitrite to produce CO_2 and N_2 (eq. 3) came from genome sequencing, whole-cell transcriptomic and proteomic analyses, and complementary physiological experiments using stable isotopes [18]. Initially, genome sequencing results were puzzling. *M. oxyfera* lacks the N_2-forming key enzyme in the denitrification pathway, nitrous oxide (N_2O) reductase (N_2OR) (see Chapter 8 of ref. [138]). At the same time, the full complement of the aerobic methane oxidation pathway was present in the genome of *M. oxyfera*. These contradictory findings could be resolved by the observation that the organism produced oxygen derived from nitrite during its metabolism [18]. The metabolic model that is consistent with all findings thus far is shown in Figure 2.

The central proposition of the model is that *M. oxyfera* harbors a nitric oxide reductase- (NOR) like enzyme that does not reduce NO into N_2O, as common NORs do (see Chapter 4), but that disproportionates NO into N_2 and O_2. The nature of this NO dismutase (NOD) and other NOR-like proteins found in the genome of *M. oxyfera* is the subject of Sections 4.1.2, 4.1.3, and 4.1.4. The production of O_2 serves the activation of methane into methanol that is oxidized to CO_2 thereby generating the electrons for methane monooxygenation and nitrite reduction (Section 4.2). One may note from Figure 2 that the substrate and electron flows are not balanced. The conversion of 8 molecules of nitrite requires the input of eight

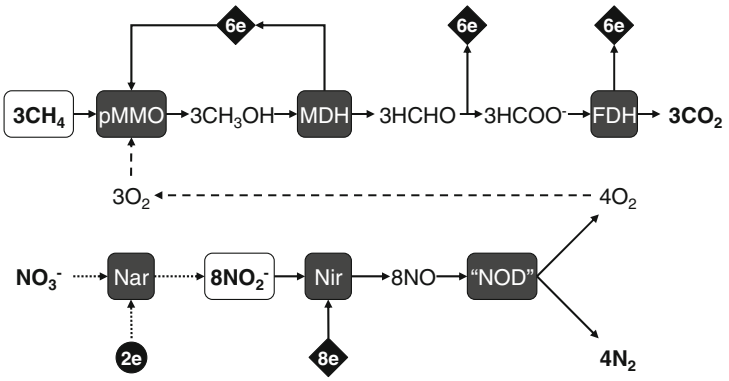

Figure 2 Scheme of the nitrite-dependent process of anaerobic methane oxidation (N-DAMO). Primary substrates, nitrite (NO_2^-) and methane (CH_4), are indicated by the rounded squares. Reactions catalyzed by metal enzymes are highlighted by dark grey squares. One may note that nitrite-dependent methane oxidation according to eq. (3) gives a surplus of one O_2 and four electrons that are converted into two water molecules. Nitrate-dependent methane oxidation (eq. 4) is only feasible with an additional external electron donor (black circle; see text). Abbreviations: FDH, formate dehydrogenase; MDH, methanol dehydrogenase; Nar, nitrate reductase; Nir, nitrite reductase; NOD, nitric oxide dismutase; pMMO, particulate methane monooxygenase.

electrons, at which four O_2 and four N_2 molecules are produced. Three O_2 molecules are required for methane activation, whilst a net 12 electrons are released in the oxidation pathway. The residual O_2 molecule and four electrons are respired into water [29]. By the same argumentation it is seen that nitrate-dependent methane oxidation by *M. oxyfera* alone (eq. 4) is not feasible for two reasons. At one hand, the conversion of eight molecules of NO_3^- would generate only four O_2 molecules, which does not sustain the monoxygenation of five CH_4 molecules. On the other hand, the oxidation of five molecules of methane generates an insufficient amount of electrons (20) for the reduction of eight molecules of nitrate into NO (24). Therefore, *M. oxyfera* has to rely on a (methane-oxidizing) nitrate-reducing partner that supplies N-DAMO with a certain amount of nitrite (or electron donor) to balance its substrate and electron flows. In the original N-DAMO enrichment culture on methane and nitrate [16] mentioned in the Introduction, this nitrite might have been supplied by the archaeal members of the culture.

3 Enzymes in Anammox Metabolism

3.1 Nitrite Reduction to Nitric Oxide

Even though it is well established that NO is an intermediate in anammox metabolism [22], it is less clear which enzyme catalyzes the reduction of nitrite into NO. In nature, two different and well investigated metalloenzymes are widely available

that catalyze the reduction: The iron- and heme *d*-containing cytochrome cd_1 (NirS), and the copper-containing NirK [30] (eq. 5).

$$NO_2^- + 2\ H^+ + \mathbf{e}^- \rightarrow NO + H_2O \quad (E_0' = +0.38\,V) \tag{5}$$

The genome of *Kuenenia stuttgartiensis*, the organism that has been used for most studies, contains a gene cluster (kuste4136-4140) encoding the full complement of a functional NirS [21, 22]. In the kuste4136 gene product all structural and functional amino acids are completely conserved with respect to NirS having a known crystal structure [31]. Kust4137 codes for a *c*-type heme (NirC) that might act as the one-electron shuttle in nitrite reduction. The gene products of kuste4138-4140 share significant sequence identities with NirN, NirJ, and NirF, respectively, known to be involved in the assembly of the heme *d* prosthetic group and further maturation of NirS [32]. However, NirS (kuste4136) and NirC (kuste4137) seem to be hardly expressed in the transcriptome and the whole-cell proteome [21, 22]. In striking contrast, NirS is among the highest expressed proteins in the marine anammox species *Scalindua profunda* [33]. Unlike the two species mentioned, anammox strain KSU-1 [34] and *Jettenia asiatica* [35] lack cyt cd_1 nitrite reductase, but they encode and express the copper-containing NirK. More surprising is the absence of both NirS and NirK in the genomes of *Brocadia* species ([36]; M. Oshiki and D. Speth, personal communication), even though cell free systems of *Brocadia sinica* display nitrite-reducing and NO-producing activity that easily supports metabolic requirements. Thus, *Brocadia* and possibly also other anammox species must have a nitrite reductase different from known NirS and NirK.

3.2 Hydrazine Synthesis

Hydrazine synthesis is the exemplary invention of anammox bacteria. The presence of hydrazine synthase enables anammox bacteria to convert ammonium anaerobically, thus providing for these organisms a specific and important niche in microbial ecosystems. Besides this, hydrazine synthase is the second enzyme, next to NOR (see Chapter 4 of this Volume), that is able to forge an N-N bond. Direct purification from *K. stuttgartiensis* identified HZS as the heterotrimeric gene products of kuste2859-2861 [22], as predicted before [21]. In this organism, HZS comprises no less than ~20 % of the cellular proteins. The kuste2859-2861 genes form part of a larger gene cluster (kuste2854-2861) of which the other genes may encode additional protein components that are needed for HZS expression and activity (Figure 3a). Kuste2857 that codes for a sigma 54-type transcriptional regulator is conspicuous in the expression regulation respect.

HZS catalyzes hydrazine synthesis from ammonium (or ammonia) and NO with the input of three electrons (eq. 6). Experiments with purified enzyme confirmed this reaction [22]. However, *in vivo* rates were exceedingly low ($20\ nmol \cdot h^{-1} \cdot mg^{-1}$ protein) and enzyme activity needed the presence of one of

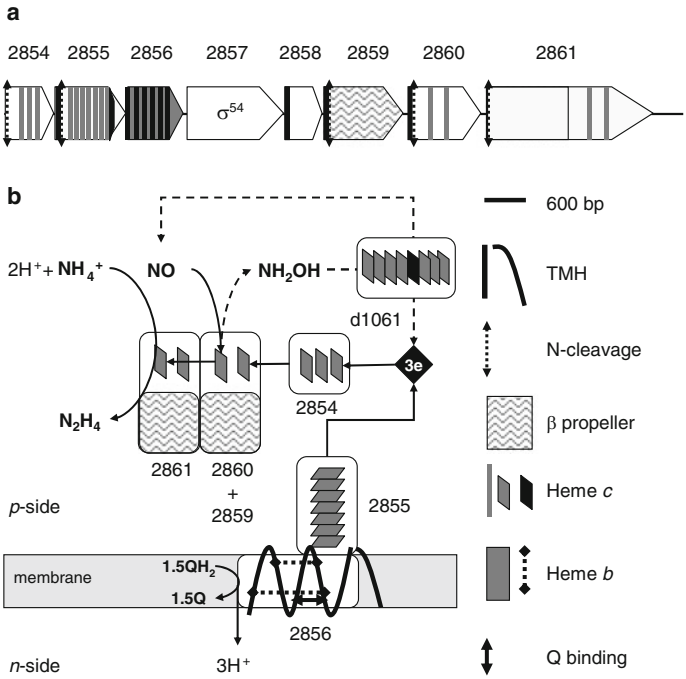

Figure 3 The hydrazine synthase system in *Kuenenia stuttgartiensis*. (**a**) Gene cluster organization. Gene lengths and the position of structural motifs are drawn to scale (bp, base pairs). Gene and protein identifiers (kuste numbers) are placed on top of the genes and next to their gene products. (**b**) Proposed functional organization of the gene products. Putative heme *b*- and menaquinone (Q)-binding sites in kuste2856 were suggested by sequence comparison with the highly homologous γ subunit (FdnI, b_{556}) of menaquinone-dependent formate dehydrogenase (FdhN) from *Escherichia coli* [40]. Possible recycling of spilled hydroxylamine during hydrazine synthesis by the action of the hydroxylamine oxidoreductase-like kustd1061 is indicated by dashed lines. Structural motifs are specified in the figure. Abbreviations: N-cleavage, N-terminal signal sequence cleavage site; TMH, transmembrane-spanning helix.

the HAO-like proteins (kustc1061) described next to artificially pull the reaction by removing the product (hydrazine) and push it by providing electrons via bovine heart cytochrome *c*. Still, *in vitro* rates were only about 1 % of *in vivo* rates. This loss in activity was already obtained by merely breaking the cells, indicating the disruption of a tightly coupled enzyme system and the requirement of other physiological relevant electron and substrate carriers. Nevertheless, HZS would be a very slow enzyme, also when fully active, possibly explaining the slow growth rate of anammox bacteria.

$$NO + NH_3 + 3\ H^+ + 3\ \mathbf{e}^- \rightarrow N_2H_4 + H_2O \quad (E_0{}' = +0.06\,V) \qquad (6)$$

$$NH_2OH \rightarrow NO + 3\ H^+ + 3\ \mathbf{e}^- \qquad (E_0' = -0.03\,V) \tag{7}$$

$$N_2H_4 \rightarrow N_2 + 4\ H^+ + 4\ \mathbf{e}^- \qquad (E_0' = -0.75\,V) \tag{8}$$

$$NH_2OH + NH_3 \rightarrow N_2H_4 + H_2O \qquad \left(\Delta G^{0\prime} = -38\,kJ \cdot reaction^{-1}\right) \tag{9}$$

Isolated HZS also catalyzes the oxidation of hydroxylamine (~1 $\mu mol \cdot min^{-1} \cdot mg^{-1}$ protein; eq. 7) and of its own product, hydrazine (34 $nmol \cdot min^{-1} \cdot mg^{-1}$; eq. 8) with rates that are one to five orders of magnitude higher than physiological hydrazine synthesis. At this stage, our understanding of the molecular mechanism underlying hydrazine synthesis is hidden in a cloud of questions. The initial biochemical characterization of the enzyme [22] and structural properties predicted from the kuste2859-2861 gene products [12, 26] might allow a first glance into this cloud (Figure 3b).

All three kuste2859-2861 genes are preceded by N-terminal signal sequences and lack any other coding sequences for transmembrane helices (TMHs), indicating the export of processed proteins across a cell membrane. In agreement herewith, antibodies raised against specific peptides localize HZS exclusively in the anammoxosome [24]. Sequence analysis suggests kuste2859 to be composed entirely of β propeller strands. In *S. profunda*, the kuste2859 and kuste2860 homologs are fused (scal00025) [33]. Also kuste2861 consists mainly of β propeller sheets, notably in its N-terminal part. In its C-terminus, two heme *c* binding motifs (CXXCH) are present. Kuste2860 contains two heme *c* binding motifs as well and sequence comparison affiliates this protein with two well-characterized enzymes with completely different functions: Cytochrome *c* peroxidase [37] and the MauG protein [38]. Cytochrome *c* peroxidase mediates the reduction of hydrogen peroxide; MauG catalyzes the intricate insertion of oxygen atoms into a precursor of tryptophan tryptophylquinone, the cofactor of methylamine dehydrogenase. Cyt *c* peroxidase and MauG harbor two *c*-type hemes each, one low-spin heme acting in electron transfer and one high-spin heme representing the catalytic center. These high-spin hemes are known to bind NO [39]. By homology, kuste2860 is inferred to be an NO-binding catalytic subunit. Binding of NO together with the addition of three electrons as proposed in Figure 3, would reduce NO to hydroxylamine (reversed reaction 7). The observed hydroxylamine oxidizing activity of HZS is consistent with this proposal. Next, the condensation of NH_2OH and ammonia together with the withdrawal of water would produce hydrazine (eq. 9). Although hydrazine synthesis in this way is exergonic *per se*, it will not be an easy reaction, taking into account the high dissociation energy of the N-H bond. To overcome the energy barrier, one might envisage the presence in HZS of a second catalytic site in which a strong oxidizing group binds ammonia to weaken the N-H bonds.

As a part of the kuste2854-2861 gene cluster, kuste2854 encodes an exported soluble triheme cyt *c* protein, which would make it an excellent three-electron carrier in hydrazine synthesis (Figure 3b) [26]. Kuste2855 codes for a protein with seven *c*-type hemes that, after export out of cytoplasm remains bound to the

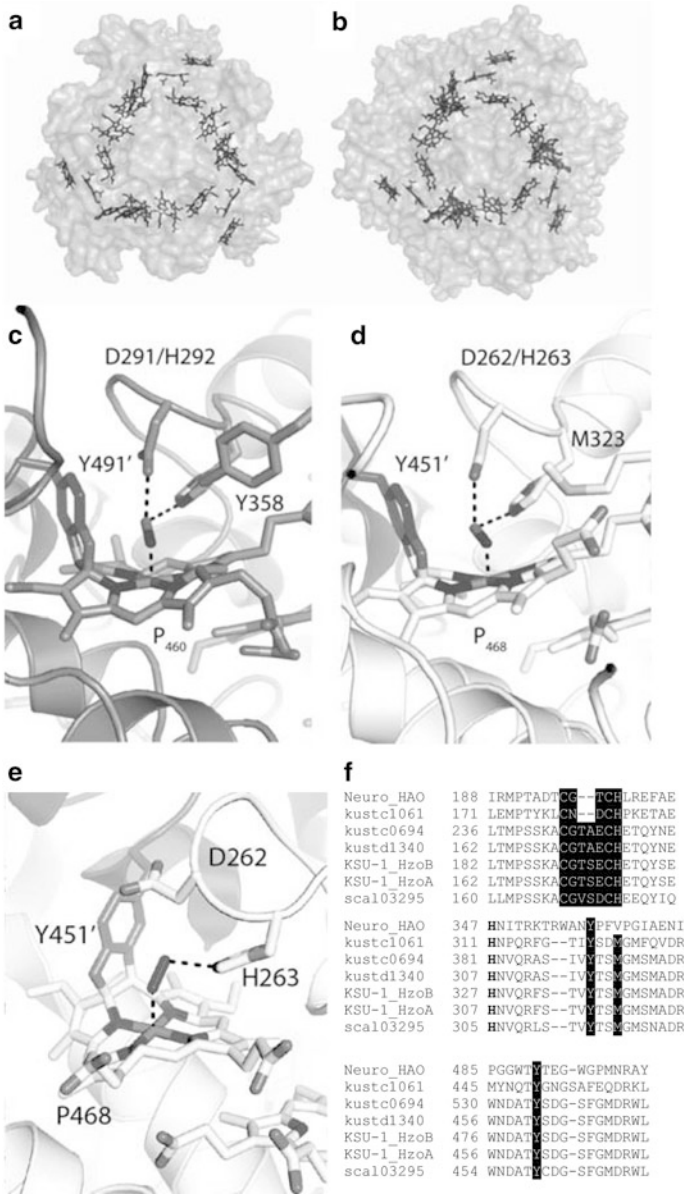

Figure 4 Structures of the homotrimeric octaheme proteins hydroxylamine oxidoreductase from *Nitrosomonas europaea* (NeHAO) and hydroxylamine oxidase kustc1061 from *Kuenenia stuttgartiensis*. Panels (**a**) and (**b**) show the conserved spatial arrangement of the 24 *c*-type hemes in NeHAO and kustc1061, respectively, as seen from the bottom of the enzymes. Panels (**c**) and (**d**) display the conserved active site configuration at heme-4 of NeHAO and kustc1061, respectively, in crystals soaked with hydroxylamine. One may note the tyrosine (Y491' and Y451') from a neighbouring subunit that makes two covalent bonds with the heme-4 in both enzymes. NeHAO (**c**) harbors an additional tyrosine (Y358) near the active site that is replaced at this

(anammoxosome) membrane by one TMH in its C-terminus. The membrane-bound kuste2856 shares significant sequence identity to the heme *b*-containing γ subunit (FdnI, cyt b_{556}) of menaquinone (MQ)-dependent formate dehydrogenase (FDH-N, FdnGHI) [26]. Sequence identity includes the conservation of the topology of the TMHs and of amino acids that are involved in binding of the two heme *b* groups and of menaquinone in the FDH-N crystal structure [40]. Herewith, kuste2855, perhaps in concert with kust2856, could act as a quinol:cyt *c* oxidoreductase at which the soluble kuste2854 shuttles the electrons to HZS (Figure 3b). The absence of this membrane system in experiments with purified HZS could be an explanation for its observed low activity [26].

3.3 Anammox and Its Multiple Hydroxylamine Oxidoreductase-Like Proteins

3.3.1 A Collection of Hydroxylamine Oxidoreductase-Like Proteins

The identification of hydrazine as an intermediate in the anammox process immediately suggested a candidate enzyme that could oxidize the compound into N_2 (eq. 8) [21]. It has been known for a long time that hydrazine can be oxidized efficiently by hydroxylamine oxidoreductase (HAO) from aerobic ammonium oxidizers [41]. In these organisms, the physiological reaction of HAO is the four-electron oxidation of hydroxylamine into the endproduct nitrite (eq. 10) [42].

$$NH_2OH + H_2O \rightarrow NO_2^- + 5\,H^+ + 4\,\mathbf{e}^- \quad (E_0' = +0.065\,V) \qquad (10)$$

HAO from *Nitrosomonas europaea* (NeHAO) has been well characterized over many years and its crystal structure is known [43, 44]. NeHAO is a homotrimeric protein in which each subunit binds eight *c*-type hemes (Figure 4a). Seven of these hemes are low-spin by proximal and distal histidine ligations. Together, they represent an electron-wiring circuit to the subunit's exit and to a next subunit. The catalytic center is heme-4 that binds and converts hydroxylamine at the distal position (Figure 4c). A remarkable property of NeHAO is the presence of two covalent

Figure 4 (continued) position by a methionine (M323) in kustc1061 (**d**). (**e**) Crystals of kustc1061 soaked in hydrazine reveal the presence of a diazene (NH=NH)-like molecule bound to the heme-4 iron. Multiple amino acid sequence alignments (**f**) of NeHAO, kustc1061 and the hydrazine dehydrogenase/oxidase (HDH/HZO) octaheme proteins from *K. stuttgartiensis* (kustc0694, kustd1340), anammox strain KSU-1 (HzoB, HzoA) and *Scalindua profunda* (scal03295) highlight the typical CX_4CH heme-3 binding motif in the HDHs (top), the active site tyrosine in NeHAO that is replaced by a methionine by a two-amino acid contraction in the anammox proteins (middle), and the conserved tyrosine that is covalently bound to the catalytic heme-4 in these octaheme proteins (bottom). Structural figures were prepared in PyMOL [48] using the following protein database (PDB ID) files: (a) 4N4N, (b) 4N4J, (c) 4N4O, (d) 4N4K, and (e) 4N4L [44].

bonds between a tyrosine from the next subunit and the active-site heme-4, constituting the P460 prosthetic group. The group is named after its specific absorption maximum around 460 nm in the fully reduced protein. Through these bonds, all three subunits are covalently linked as a 200 kDa complex. For as-yet not fully understood reasons, the P_{460}-type heme favors substrate oxidation reactions [45]. In contrast, other related multiheme proteins that lack the tyrosine heme-4 crosslink are equipped for reductive substrate conversions.

Rather than one, no less than ten different HAO paralogs are detected in the genome of *K. stuttgartiensis*, six of which being highly expressed at the transcriptome and proteome levels (Figure 5) [21, 22]. The collection of HAO-like proteins is highly conserved in other genomes of anammox bacteria as well. The straightforward questions then were, which one(s) would be the physiological hydrazine dehydrogenase(s), what would the others do, and how would the different HAO paralogs be tuned to a presumably specific function? Sequence comparison and phylogenetic analysis allow their classification into a number of subgroups (Figure 5) [12, 26, 45]. Four of the proteins (kustc0694, kustd1340, kustc1061, and kusta0043) possess the tyrosine in their C-terminus that makes the covalent bonding in HAO. Six of these lack the particular tyrosine, at which kustc0458, kuste4574, and kuste2479 cluster as one subgroup sharing ~50 % sequence identity to each other. The residual three, lowly expressed ones (kustd2021, kuste2435, and kuste2457) display less than 30 % sequence identities, both to each other and to the seven ones already mentioned. Direct evidence for the function of some HAO-like paralogs has come from direct purification and subsequent characterization.

3.3.2 Hydroxylamine Oxidation to Nitric Oxide

The best understood HAO-like protein from anammox bacteria, both regarding its structure and function, is kustc1061 from *K. stuttgartiensis* [44]. The protein has also been purified from anammox strain KSU-1 [46] and from *Brocadia anammoxidans* [47]. In agreement with what is seen in its protein sequence (Figure 5), kustc1061 is an octaheme protein in which the (three) subunits are covalently bound via the conserved tyrosine to the catalytic heme-4, like in NeHAO [44]. Despite an only 30 % sequence identity, kustc1061 and NeHAO share a highly similar overall architecture (Figure 4). The similarity encompasses the spatial position and orientation of the eight heme groups, and the structure of the P_{460} catalytic heme-4. Such heme arrangement was also found in other multiheme proteins, like cyt *c* nitrite reductase (see Chapter 9 of ref. [138]). Still, there appears to be one significant difference between kustc1061 and NeHAO, which affects the functionality of both enzymes. NeHAO contains a specific tyrosine near the catalytic site, which is absent in kustc1061 (Figures 4c and d).

Both kustc1061 and NeHAO catalyze the oxidation of hydroxylamine, but with different outcomes. While kustc1061 produces NO in a three-electron

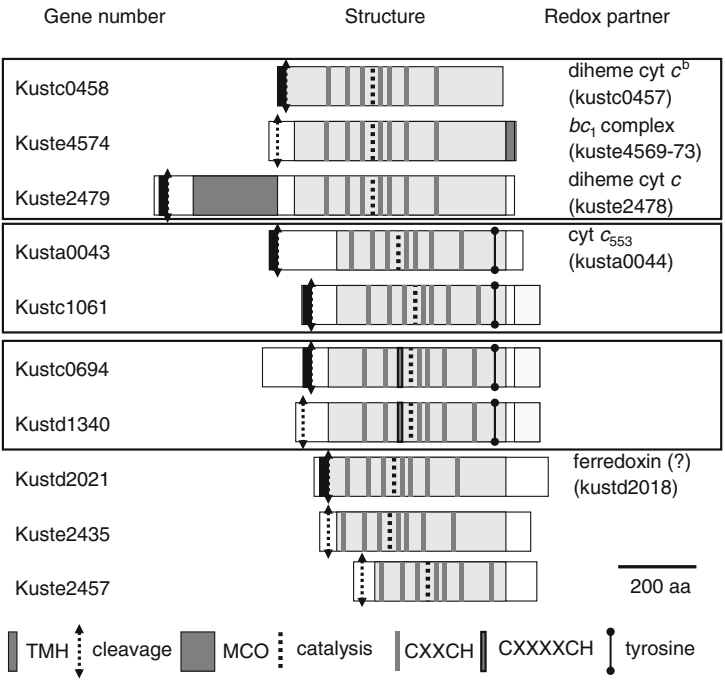

Figure 5 A family of ten hydroxylamine oxidoreductase (HAO)-like proteins in the genome of *Kuenenia stuttgartiensis* [12, 26]. Lengths of the polypeptides are drawn to scale (aa, amino acids). Homologous stretches that are rich in *c*-type hemes are vertically aligned. HAO-like proteins showing high sequence identities, suggestive of a same function, are boxed. Structural motifs are specified in the figure with the following abbreviations: TMH, transmembrane-spanning helix; cleavage, N-terminal signal sequence cleavage site; MCO, multicopper oxidase; catalysis, catalytic *c*-type heme; CXXH, heme *c*-binding motif; CXXXXCH, divergent heme *c*-binding motif; tyrosine, tyrosine involved in covalent bonding with the catalytic heme.

oxidation (eq. 7), the reaction product of NeHAO is nitrite (eq. 10). Hydroxylamine reacts spontaneously with as-isolated fully oxidized kustc1061, at which the enzyme undergoes a two-electron reduction and hydroxylamine gets oxidized to the HNO nitrosyl state. In crystals both of kustc1061 and HAO soaked with hydroxylamine, the nitrosyl is bound to the iron of the P_{460} catalytic heme [44] (Figures 4c and d). The subsequent one-electron oxidation of HNO yields NO, which is released in case of kustc1061. The sequence of events suggests the catalytic mechanism shown in Figure 6. In the reaction catalyzed by NeHAO, a water molecule has to be added to NO to produce nitrite after one more one-electron oxidation. The tyrosine next to the NeHAO catalytic site, which is absent in kustc1061, is perfectly positioned to mediate such water addition [44].

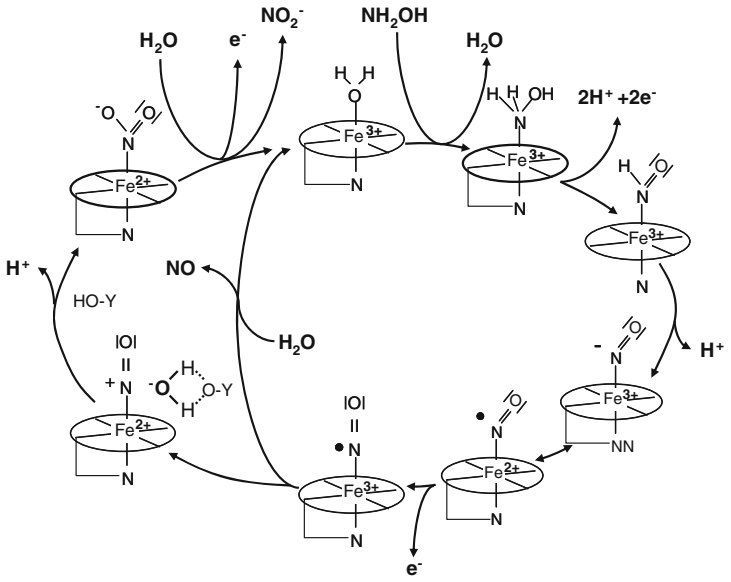

Figure 6 Reaction mechanism of hydroxylamine oxidation to nitrite by hydroxylamine oxidoreductase (HAO) (outer cycle) and to nitric oxide (NO) by kustc1061 (inner cycle). The scheme combines models proposed for the mechanism of kustc1061 [44] and of HAO ([49] and references therein) assisted by a specific tyrosine near the HAO active site for the addition of water.

Besides hydroxylamine conversion, kustc1061 catalyzes the four-electron oxidation of hydrazine (eq. 8), albeit with 50-fold lower catalytic efficiency (k_{cat}/K_m) [44]. Analogously to hydroxylamine, hydrazine added to the oxidized protein results in a diazene-like (NH=NH) molecule bound to the P_{460} iron [44] (Figure 4e). Even though hydrazine is not the physiological substrate of kustc1061, this observation might be of relevance in understanding the function of the genuine hydrazine dehydrogenase described in the next section.

It is understood by now that hydroxylamine is not an intermediate and the function of kustc1061 as a specific hydroxylamine oxidase is not easy to reconcile with anammox central metabolism as we know it. However, hydroxylamine could be an intermediate in hydrazine synthesis (see previous Section 3.2; Figure 3) and, as suggested before [26], failure to complete the difficult condensation reaction with ammonia might result in the spillage of hydroxylamine. Now, kustc1061 would expertly serve the regeneration of NO and three electrons for a next synthesis attempt. In this respect, it may be interesting to note that kustc1061 homologs in other anammox genomes are clustered with the HZS system [33–36].

3.3.3 Hydrazine Oxidation and Nitrogen Formation

Direct purification from *K. stuttgartiensis* identified the genuine N_2-forming hydrazine dehydrogenase/oxidase (HDH/HZO) as kustc0694 [22]. The homologous enzyme from anammox strain KSU-1 had been described before [50], but its function was not fully assured by then. Kustc0694 is a member of the HAO-like family introduced above (Figure 5). The purified protein is 100 amino acids shorter than annotated in the genome database because of an incorrect assignment of the start codon and N-terminal signal peptide cleavage [22]. This cleavage is most likely associated with the export of kustc0694 into the anammoxosome [24]. Kustc0694 is over 95 % identical, both at the nucleotide and amino acid levels, to kustd1340, most likely representing a second HDH in *K. stuttgartiensis* and other anammox species.

Like kustc1061 and NeHAO, kustc0694 is a homotrimeric protein carrying eight *c*-type hemes per subunit and the three subunits are covalently linked to each other [22, 50]. A peculiar feature of kustc0694 and its close homologs is the divergent CX_4CH binding motif for heme-3 (Figures 4f and 5). The rational for this is not understood. The increase in length between both cysteines that bind the heme *c* most likely affects the position of this heme with respect to neighboring hemes, in its turn affecting electron transfer between the hemes. Upon reduction of the oxidized protein, the characteristic P_{460} absorption maximum is observed [50]. This observation, the covalent binding of the subunits, and the presence in the kustc0694 sequence of the tyrosine that makes two bonds to heme-4 in kustc1061 and NeHAO (Figure 4) are highly suggestive that heme-4 is the catalytic site also in kustc0694.

Kustc0694 catalyzes with high V_{max} and low K_m the four-electron oxidation of hydrazine to N_2 according to equation 8 [22]. Hydroxylamine is not a substrate, but rather a strong competitive inhibitor with respect to hydrazine. Also NO, a free intermediate in anammox metabolism, competitively inhibits hydrazine oxidation with low K_i. Incubation of kustc1061 with hydrazine results in the two-electron-oxidized diazene bound to the P_{460} heme (Figure 4e). Although this remains to be shown, the same could hold for kustc0694. The subsequent two-electron oxidation of diazene would then make N_2. The passage of two times two electrons through an electron wire composed of a series of one-electron (heme) carriers will need a fine-timing of the electron circuit. Similarly, the P_{460} catalytic center has to be fine-tuned for hydrazine turnover. How these aspects are resolved is a matter of ongoing research, which will include the resolution of the kustc0694 crystal structure. Future investigations have to address one more important issue, namely how the low-redox potential electrons derived from hydrazine oxidation (eq. 8) are utilized to build up a proton-motive force.

3.3.4 What About the Other Hydroxylamine Oxidoreductase-Like Proteins?

Kustc0458, kuste4574, and kuste2479 share significant sequence identities, especially regarding the presence and the position in their protein sequences of eight *c*-type hemes (Figure 5). This might suggest that these three proteins have a

similar function. All three lack the tyrosine in the C-terminus, which is responsible for the binding with a catalytic heme, indicative of reductive transformations [45].

Kustc0458 has been purified from K. *stuttgartiensis* and its crystal structure has been resolved as a heterododecameric ($\alpha_6\beta_6$) complex composed of a dimer of kustc0458 octaheme trimers at which each kustc0458 subunit is associated with the diheme kustc0457 [51]. Altogether, the complex harbors no less than sixty *c*-type hemes. Again, the catalytic center is heme-4, but this heme is not covalently bound to a next subunit. Correspondingly, the kustc0457-0458 complex does not catalyze the oxidation of nitrogenous substrates and the only activity that could be measured was the reduction of nitrite, presumably to ammonium [51]. However, this activity was obtained with reduced methyl viologen as a powerful reductant. Since reduced viologen dyes also support reductive reactions by NeHAO [52] and kustc1061 [44] artificially, the question remains if nitrite reduction to ammonium represents the physiological reaction of kustc0457-0458. An answer to this question may be found by the isolation and identification of the physiological electron carrier of the complex. Here, an attractive candidate would be the gene product that is directly linked to the kustc0457 and kustc0458 genes, namely kustc0456. Sequence analysis identifies kustc0456 as a novel type-1 copper-containing cupredoxin [26]. Cupredoxins serve as electron carriers in many respiratory and photosynthetic systems [53], including NO-forming nitrite reductase NirS [54].

Kustc0458 shows 47 % sequence identity to kuste4574 (Figure 5). The identity comprises the conservation in the alignment of the eight heme-*c* binding sites including six or seven histidines that make up the distal ligands to the electron-wiring *c*-type hemes, leaving heme-4 as the catalytic site also in kuste4574. As already mentioned, kuste4574 lacks the tyrosine that is involved in the covalent bonding of heme-4 in NeHAO, kustc0694, and kustc1061, indicative of a reductive catalysis. Importantly, kuste4574 forms part of a gene cluster (kuste4569-74) that codes for one of three bc_1 complexes in *K. stuttgartiensis* (Figure 7) and this bc_1 complex could be most remarkable by its composition.

Like canonical bc_1/b_6f complexes, the kuste4569-74 genes code for a 2Fe-2S Rieske subunit (kuste4569), a heme *b*- and quinone-binding part (kustc4571-72) and a *c*-type heme (kuste4573). However, detailed sequence analyses affiliate this anammox system, as well as the alternative system encoded by kustd1480-85, with a novel type of *bc* complexes [55, 56]. The Rieske subunit could have aberrant redox properties [55], the heme *b*- and quinone-binding part is split across two proteins similar to photosynthetic b_6f systems, and the *c*-type heme is a hexaheme protein. Besides HAO-like kuste4574, kuste4569-74 gene cluster codes for one more polypeptide, an FAD-binding NAD(P)H oxidoreductase (kuste4570). If assembled as one whole, the question is what the complex would do, and an answer can only be a speculative one: The simultaneous coupling by a bifurcation mechanism of (mena)quinol oxidation to the reduction of both a nitrogenous substrate and $NAD(P)^+$ [26]. If the reduction encompasses the conversion of nitrite into NO, this would answer two open issues at the same time, the nature of the elusive nitrite reductase and the way NAD(P)H is generated for biosynthetic purposes.

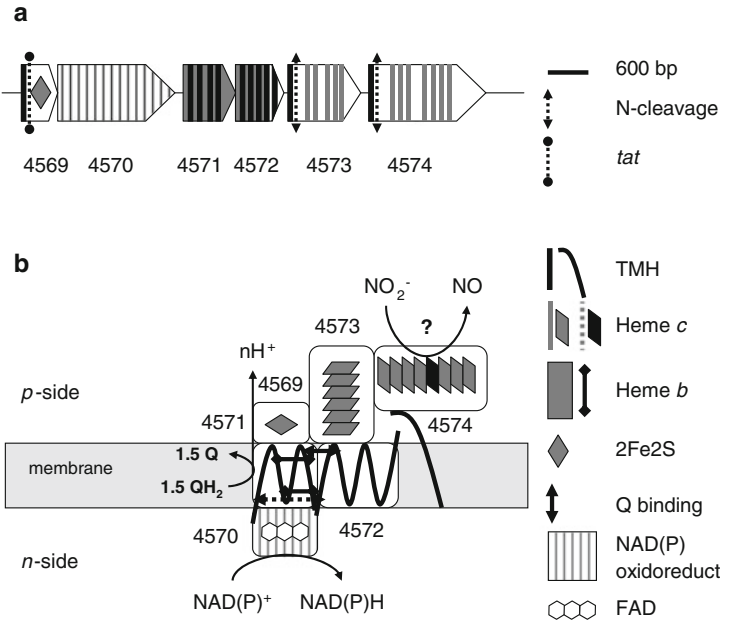

Figure 7 Gene cluster organization (**a**) and possible functional organization of its gene products (**b**) of a novel cytochrome *bc* complex found in anammox bacteria. The complex consists of Rieske-type 2Fe2S iron sulfur protein, a membrane-bound heme *b* part split across two proteins and a *c*-type cytochrome [12, 26] together with a HAO-like octaheme protein and a FAD-dependent NAD(P)H oxidoreductase. Heme *b*- and quinone (Q)-binding sites were inferred from the conservation of amino acids in crystal structures of bc_1 and b_6f complexes implicated in the binding of these compounds [57]. The anammox *bc* complex has been suggested to couple menaquinol oxidation to the reduction of nitrite and $NAD(P)^+$ by a bifurcation mechanism [26]. Numbers in (a) and (b) refer to the gene identifiers (kuste) of *Kuenenia stuttgartiensis*. Gene lengths and the position of structural motifs are drawn to scale (bp, base pairs). Structural motifs are specified in the figure. Abbreviations are the following: N-cleavage, N-terminal signal sequence cleavage site; *tat*, twin-arginine translocation signal; TMH, transmembrane-spanning helix.

Kuste2479 is another interesting HAO-like protein that is well conserved amongst anammox bacteria. While its C-terminal part with its eight *c*-type hemes shows significant (>50 %) sequence identity to kustc0458 and kuste4574, the N-terminal sequence is comprised of a leader sequence for protein export and an amino acid sequence that maps to the broad family of copper-containing laccases [58], and to two-domain small laccases more specifically [59]. The neighboring gene kuste2479 codes for a diheme protein in the N-terminus and a linocyn in the C-terminus. Linocyns assemble into isohedral nanocompartments that enclose oxidative-stress response proteins [60]. After export out of the cell, the assembly might act in the removal of reactive oxygen or nitrosative species. The presence and identification of such nanobodies in anammox cultures remains to be established, which will not be an easy task since kuste2479 and kuste2478 are only lowly expressed.

3.4 The Oxidation of Nitrite and Reduction of Nitrate

3.4.1 The Nitrite:Nitrate Oxidoreductase System

In anammox metabolism, the nitrite:nitrate oxidoreductase (NXR) serves two opposite goals, (1) the oxidation of nitrite to replenish the cyclic electron flow upon draining due to the loss of intermediates (NO, hydrazine) or electrons for biosynthetic activities, and (2) the reduction of nitrate to nitrite during growth in the presence of external electron donors other than ammonium (eq. 11) (Figure 1). In *K. stuttgartiensis*, structural genes (*NxrABC*) coding for the NXR protein form part of a large gene cluster (kustd1699-1713), which is highly conserved among anammox genomes.

$$NO_2^- + H_2O \rightleftharpoons NO_3^- + 2\,H^+ + 2\,\mathbf{e}^- \quad (E_0' = +0.43\,V) \tag{11}$$

The cluster encodes an astonishing range of metal-containing proteins (Figure 8a). The *NxrABC* structural genes are represented by kustd1700, kustd1703, and kustd1704, respectively. Herein, kustd1700 codes for a protein (1148 amino acids) that is preceded by a twin-arginine translocation (*tat*) signal for protein export and that belongs to the broad class of molybdopterin (MPT) enzymes. Members of this class catalyze a variety of oxidation and reduction reactions of N-, S- or carbon-substrates (see [61] for a review). Amongst many others, the family includes nitrate reductase (NarGHI), formate dehydrogenase (see Section 4.2.4), acetylene hydratase (see Chapter 2 of ref. [138]), and dimethylsulfoxide (DMSO) reductase and dimethylsulfide dehydrogenase (see Chapter 11 of ref. [138]). Quite a few MPT proteins have been well characterized by the resolution of their atomic structures [61]. Their common property is the presence of a catalytic molybdenum atom that is coordinated by four sulfur atoms derived from two antiparallel-oriented dithiolene-containing pterins that are esterified with guanine dinucleotide (Mo-*bis*PGD) (Figure 8b). The pterin occurs in two conformers, as a tricyclic (pyranopterin) and a bicyclic structure with an open furan (molybdopterin). A fifth ligand to molybdenum is provided by a serine, cysteine, selenocysteine, or a mono-/bidentate oxo/hydroxyl group (D222 in NarG) [62]. In the N-terminal part, a conserved set of cysteines is usually present to bind a 4Fe4S cluster (FS0). While sequence analysis unambiguously identifies kustc1700 as a molybdopterin protein, sequence identity with MPT enzymes of known function, including NarG nitrate reductase, is moderate (10–25 %). By and large, kustd1700 harbors the series of amino acids that have been identified in other MPT proteins with the binding of the Mo-*bis*PGD cofactors, but the full conservation with any known protein is not seen. This would imply that Mo and its cofactors are bound such as to facilitate its specific catalytic function, the oxidation of nitrite to nitrate. In agreement herewith, sequence identity is highest (~60 %) with putative *Nxr* genes found in the genomes of the nitrite oxidizers *Candidatus* 'Nitrospira defluvii' [63] and *Nitrospina gracilis* [64]. Despite the overall divergence, kustd1700

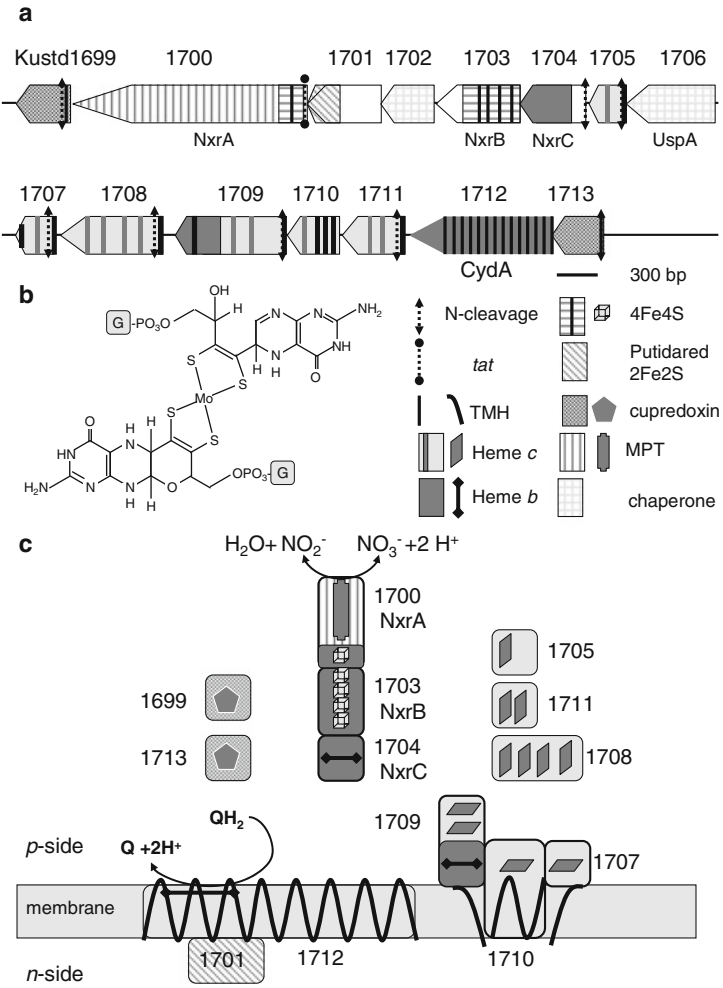

Figure 8 Gene cluster organization (**a**) and possible functional organization (**c**) of the nitrite: nitrate oxidoreductase (NXR) system in *Kuenenia stuttgartiensis*. Numbers in (a) and (c) refer to the gene identifiers (kustd) of *Kuenenia stuttgartiensis*; gene lengths and the position of structural motifs in (a) are drawn to scale (bp, base pairs). Structural motifs are specified in the figure. The system is suggested to be comprised of the catalytic NxrABC protein, membrane-bound protein complexes, including a protein (kustd1712) partly related to subunit I (cydA) of the cytochrome *bd* quinol oxidase (CydAB) [71] and several heme-*c* type as well as novel cupredoxin-type [26] soluble electron carriers. NxrA houses a Mo-*bis*(pyrano guanine dinucleotide) cofactor common to all molybdopterin enzymes of which the chemical structure is shown in (**b**). In this structure the open furan form of the pterin moiety is displayed above and the tricyclic pterin below the molybdenum that is coordinated by the dithiolene groups; G, guanine monophosphate. Putative heme *b*- and quinone (Q)-binding sites were inferred from the CydAB sequence [71]. Abbreviations: N-cleavage, N-terminal signal sequence cleavage site; *tat*, twin-arginine translocation signal; TMH, transmembrane-spanning helix; putidared, putidaredoxin-like 2Fe2S iron sulfur cluster; MPT, Mo-*bis*(pyrano guanine dinucleotide) cofactor; UspA, universal stress protein A.

contains the aspartate (D222) that binds Mo in NarG. Also the set of FS0-binding cysteines is found, albeit with one remarkable difference. In NarG the iron sulfur cluster is coordinated by a $HX_3CX_3CX_{34}C$ sequence [62, 65], whereas a $CX_3DX_3CX_{39}C$ sequence is found at this position in kustd1700 and homologous nitrifier sequences. The difference in coordination likely will affect the redox potential of the FS0 iron-sulfur cluster in its role to transfer electrons to or from the molybdopterin catalytic site.

Like in many MPT proteins [61], electron transfer encompasses a second subunit (NxrB, kustd1704) that contains the conserved set of cysteines to accommodate 4 additional iron sulfur clusters (FS1-4), in which FS1-3 represent 4Fe4S clusters and FS4 is a 3Fe4S moiety. Unlike archetypal MPT proteins [61], the third subunit (NxrC, kustd1704) is not a membrane anchor. Rather, kustd1704 is a soluble protein with an N-terminal signal sequence for protein export (Figure 8). Importantly, NxrC shares highest sequence identity with the heme *b*-containing C subunits of a subset of MPT proteins, as there are dimethylsulfide dehydrogenase [66], selenate reductase [67], chlorate reductase [68], and ethylbenzene dehydrogenase [69]. Sequence identity includes the amino acids that coordinate heme *b* in the crystal structure of ethylbenzene dehydrogenase [69].

Besides the three structural subunits, the kustd1699-1713 gene cluster encodes a series of other proteins that apparently play a role in the functioning of the NXR system. The gene product of kustd1702 is related to the NarJ and TorD proteins that act as chaperones in MPT protein maturation [70]. A chaperone role is also anticipated for the universal stress protein A (UspA)-related kustd1706. Kustd1701 is characterized by four C-terminal cysteines with the typical spacing of adrenodoxin/putidaredoxin-like 2Fe2S clusters. Kustd1707, kustd1710, and kustd1709 have one or more TMHs at which the former two carry one *c*-type heme each with an orientation as proposed in Figure 8c. Kustd1709 is remarkable by its fusion of heme *b*-containing kustd1704 and kustc0457, found as the diheme subunit of the kustc0457-0458 complex described above (see Section 3.3.4). It is conceivable that these three membrane-associated proteins form a complex, possibly associated with one or more of the remaining polypeptide components of the kustd1699-1713 gene cluster. Herein, kustd1712 would be membrane-bound by no less than 15 predicted TMHs. The first N-terminal half of kustd1712 displays significant sequence identity with the quinone- and heme *b*-binding subunit (CydA) of cytochrome *bd* oxidase (CydAB) [71]. Kustd1705, kustd1708, and kustd1711 again are preceded by N-terminal cleavage sites and possess CXXCH motifs for the binding of one, four, and two *c*-type hemes, respectively. In front and at the end of the kustd1699-1713 cluster, two genes are found that encode exported proteins with type-1 cupredoxin features that are homologous to kustc0456 encountered before (Section 3.3.4). Together, these proteins provide an array of mobile and membrane-bound carriers that somehow are involved in electron and possibly proton-translocating processes related with nitrite oxidation and nitrate reduction. However, the specific role of each of them remains to be established.

3.4.2 Nitrite Reduction to Ammonium

In the presence of inorganic electron donors such as Fe(II) compounds, Mn^{2+} and possibly dihydrogen, or organic compounds, most notably formate, acetate or propionate, anammox bacteria may adopt a lifestyle "disguised" as denitrifier [28]. Different species may even have specialized in the use of certain electron donors, providing them a competitive advantage. For instance, *Candidatus* 'Brocadia fulgida' was specifically enriched in a medium that contained ammonium and nitrite supplemented with a low (1 mM) concentration of acetate [28]. In contrast, *Candidatus* 'Anammoxoglobus propionicus' came to the fore under the same enrichment conditions and with the same inoculum, except that propionate substituted for acetate [28]. As outlined in Section 2.1, during "disguised" denitrification half of nitrite is reduced to ammonium, which combines with the other half to produce dinitrogen gas in the anammox process (Figure 1). Consequently, all N_2 is produced from nitrite or nitrate, as is also the case with "true" denitrification. The key enzyme in "disguised" denitrification would be the nitrite reductase making ammonium. This is also the key enzyme in the so-called DNRA bacteria that make a living from the dissimilatory nitrite/nitrate reduction to ammonium.

$$NO_2^- + 8\ H^+ + 6\ \mathbf{e}^- \rightarrow NH_4^+ + 2\ H_2O \quad (E_0' = +0.43\,V) \tag{12}$$

DNRA bacteria occur in broad and likely only partly appreciated diversity of species in many ecosystems where they make a short circuit in the N-cycle [72]. The organisms use nitrite as terminal electron acceptor, which is reduced by the input of six electrons to ammonium without the release of intermediates (eq. 12). This type of nitrite respiration is mediated by the NrfHA/NrfABCD systems that are discussed in Chapter 9 of ref. [138]. Briefly, NrfH is a membrane-bound tetraheme *c* protein belonging to the NapC/NirT family of menaquinol oxidases [45, 73]. NrfH accepts the electrons from menaquinol and transfers these to its associated catalytic part, NrfA. In enteric bacteria the alternative, partly soluble NrfABCD system is found in which the soluble pentaheme cytochrome *c* NrfB mediates electron transfer between the catalytic NrfA (alternatively named cytochrome c_{552} nitrite reductase) and the membrane-associated iron-sulfur protein NrfC and NrfD, which is an assumed quinol dehydrogenase of the NrfD/PsrC family [73]. Thus, NrfA represents the catalytic enzyme in both systems. NrfA is a homodimeric pentaheme cytochrome *c* protein (unrelated to NrfB) localized in the periplasm. The five *c*-type hemes (1–5) of NrfA fully superimpose hemes 4–8 of the HAO-like proteins shown in Figure 4. Heme-1 in NrfA represents the catalytic site and it is the equivalent of heme-4 in the HAOs. A distinctive feature of this heme-1 is the presence of a lysine as a proximal ligand, which is signified by the CXXCK motif in the protein sequence. The presence of the lysine seems to be a governing factor in the reactivity of NrfA, next to a conserved triad of

amino acids near the active site (R114, Y218, H277; numbering according to the *Wolinella succinogenes* structure, PDB ID 1FS7) [74].

The nature of a NrfA-like protein in anammox bacteria has been elusive for quite some time. The reason for this is that no pentaheme protein could be found in sequenced genomes with the diagnostic CXXCK motif and the RYH triad. Members of the *Campylobacteriaceae* such as *Campolybacter jejuni* [75] and *Anaeromyxobacter dehalogenans* [76] that are known for their DNRA activity lack the particular pentaheme proteins as well. However, cytochrome c_{552} nitrite reductases have been annotated in their genomes, yet bearing the common CXXCH binding motif for heme-1. Deletion and expression analyses of the alternative *Campolybacter jejuni* pentaheme protein demonstrated that it is a nitrite reductase making ammonium [77]. The alternative NrfAs remain to be characterized regarding the nature of the proximal ligand to heme-1. It is possible that this ligand is a lysine derived from another part of the protein sequence, rather than a histidine. Furthermore, detailed sequence analyses affiliated the *Campylobacteriaceae* and *A. dehalogenans* proteins with a broad class of NrfAs that covered 18 clades (A-R), three of which (J-L) being characterized by a CXXCH motif for heme-1 [78]. Importantly, close homologs of one of the three clades (K) are found in the genomes of anammox strain KSU-1 (KSU1_B0055) [34], of *Brocadia* species [36] and of *Jettenia* ([35]; D. Speth and M. Oshiki, personal communication). In these genomes, *nrfA* genes are localized next to the ones coding for tetraheme NrfH proteins. However, the genome of *K. stuttgartiensis*, which is able of ammonium formation from nitrite [28], lacks the particular homolog, as does *Scalindua*.

Besides pentaheme nitrite reductases, two different octaheme proteins are known that reduce nitrite to ammonium with high catalytic efficiencies, both of which crystal structures have been resolved: A homohexameric enzyme from *Thioalkalivibrio* species [79] and a homodimeric enzyme from *Shewanella oneidensis* [80]. Despite a limited amino acid sequence identity, the spatial arrangement of the eight hemes is highly similar in both types. In fact, heme arrangements are conserved with respect the ones of the octaheme HAO-like proteins described above (Figure 4) and of pentaheme NrfA. Like in NrfA, the catalytic hemes are proximally ligated by a lysine, albeit in different fashions. In the *S. oneidensis* enzyme, the catalytic heme-2 receives the coordinating ε-amine from a lysine in a distal part of the amino acid sequence [80], whereas the catalytic heme-4 in the *Thioalkalivibrio* proteins is lysine-coordinated by the CXXCK heme-4 binding sequence [79]. Notwithstanding the extant collection of octaheme proteins (Figure 5), homologs of those octaheme nitrite reductases are absent in genomes of anammox bacteria. Still, this does not rule out that one of the anammox HAOs fulfils a physiological function of an ammonium-forming nitrite reductase. In this respect, it is interesting to note that kustd2021 homologs (Figure 5) are consistently present in genomes that lack the alternative (CXXCH) NrfA, whereas genomes of anammox species that possess such NrfA are devoid of kustd2021 homologs.

4 Enzymes in Nitrite-Driven Methane Oxidation

M. oxyfera derives its energy for growth from the oxidation of methane coupled to the reduction of nitrite or nitrate (eqs 3 and 4). Presently, none but one of the enzymes involved in these processes has been purified and characterized. Progress in the field is severely hampered by the extremely slow growth rate and growth yield of the organism, which is enriched as tight aggregates that withstand a convenient cell breaking and protein extraction. Consequently, our knowledge on *M. oxyfera* metabolism mainly relies on what its genome tells us and what we have learned from detailed functional and structural studies on homologous enzymes from methanotrophic, methylotrophic, and denitrifying model organisms. A striking aspect of the genome of *M. oxyfera* is the redundancy of many of its catabolic enzymes [18]. In the genome, the inventory is found for two different nitrate reductases, multiple heme-copper oxidases including Nor-like proteins, three different methanol dehydrogenases, two different pathways for formaldehyde-formate interconversion and three different formate/formyl dehydrogenase systems. The rationale behind this redundancy is unclear and an answer may come only from future physiological, biochemical and perhaps genetic research.

4.1 The Nitrite Reduction Route

4.1.1 Nitrite and Nitrate Reduction to Nitric Oxide

The genome of *M. oxyfera* harbors the inventory for two different nitrate reductases, the membrane-bound NarGHI system briefly mentioned in Section 3.4.1, which is localized in the cytoplasm, and the periplasmic NapAB system [30, 81]. Both systems are well studied in denitrifiers [81], which includes the elucidation of several crystal structures [62, 65, 82]. Both systems are only lowly expressed at the transcriptome and proteome levels in *M. oxyfera*, which makes sense in enrichment cultures grown on nitrite.

In the genome of *M. oxyfera*, the NarGHI system is encoded on the DAMO_0779-0774 gene cluster (Figure 9a). Structural genes are represented by DAMO_0778 (*narG*), DAMO_0776 (*narH*) and DAMO_0774 (*narI*). The genes are interspersed by genes coding for a hemerythrin-like protein (DAMO_0777) and the common NarJ (DAMO_0775) with a chaperone function [70]. At the end of the cluster, DAMO_ 0779 codes for a *c*-type triheme protein that could be bound to the membrane by one TMH in its C-terminus. DAMO_ 0779 shows ~40 % sequence identity to proteins found in the genomes of the nitrite-oxidizing *Nitrospina* (CCQ90255) and of *Sinorhizobium fredii* (CCE99719) where it has been annotated as subunit II of cytochrome *cb* oxidase, and to the *K. stuttgartiensis* kustc0457 diheme protein described before (Section 3.3.4). Quite remarkably, NarGHI from *M. oxyfera* display highest sequence identities (~80 %) to the corresponding polypeptides from the aerobic nitrite oxidizers *Nitrococcus mobilis* and *Nitrobacter hamburgensis* that will employ their NarGHI for nitrite oxidation. Sequence identity with the NarG (45 %), NarH (51 %), and NarI (31.5 %) subunits of the

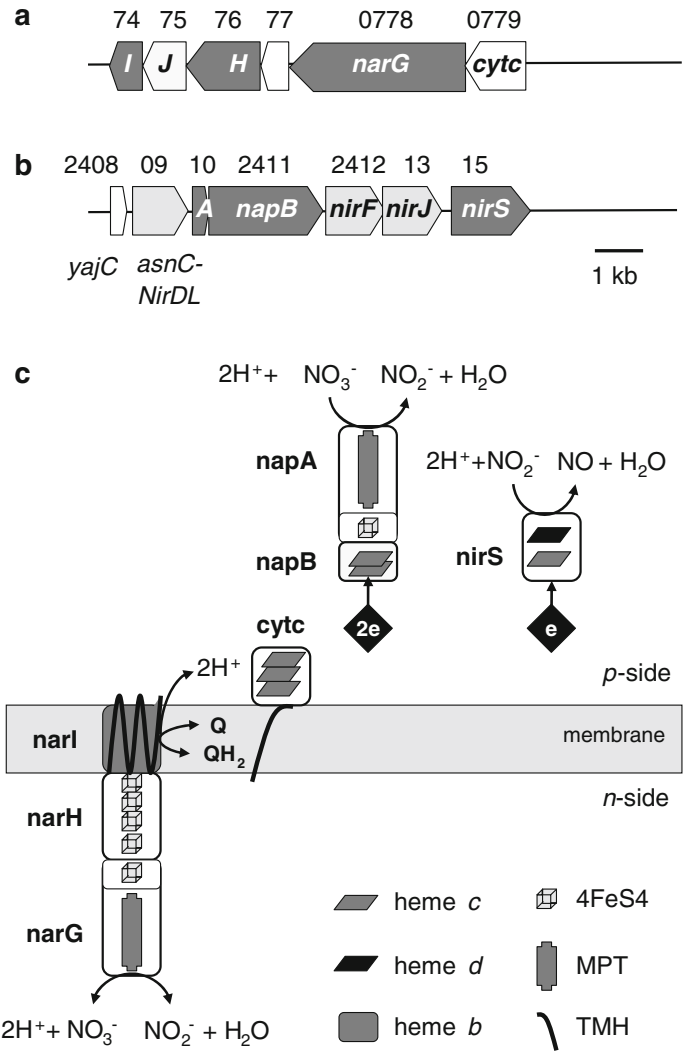

Figure 9 Gene cluster organization of (**a**) the cytoplasmic dissimilatory nitrate reductase (Nar), and (**b**) periplasmic dissimilatory nitrate reductase (Nap) and nitrite reductase (Nir) systems in *Methylomirabilis oxyfera*. Gene lengths and intergenic regions are drawn to scale. Genes coding for catalytic proteins are shaded dark grey (white lettering) and for accessory proteins light grey; see text for the function of the accessory proteins. Gene orientation is indicated by the arrow heads and numbers refer the gene identifiers (DAMO_). The localization of the enzymes systems and their putative functional organization are displayed in (**c**). Herein the *p*- and *n*-sides refer to the positive (periplasmic) and negative (cytoplasmic) sides of the cell. As yet unknown carriers that transfer electrons for nitrate and nitrite reduction are indicated by black diamonds. Structural motifs are specified in the Figure with the following abbreviations: MPT, Mo-*bis*(pyrano guanine dinucleotide) cofactor; TMH, transmembrane-spanning helix.

structurally resolved nitrate reductase from *Escherichia coli* [62, 65] is less, but all structural features are conserved in *M. oxyfera* NarGHI. Conserved features comprise domain organization of the three subunits, amino acids that bind the Mo-*bis*PGD prosthetic group and the 4Fe4S cluster in NarG, amino acids in NarH that coordinate the four iron-sulfur clusters, and those in NarI that are related with the binding of two heme *b* molecules and menaquinone. Unlike many other NarG subunits, DAMO_0778 is not preceded by a *tat* signal for protein export, but in other systems the N-terminus is protected from cleavage to leave the nitrate reductase in the cytosol [83].

Contrary to Nar, the Nap system is localized in the periplasm (Figure 9c). In its essence, the Nap system is composed of the heterodimeric NapAB in which NapA is a molybdopterin protein bearing a 4Fe4S cluster in its N-terminal region, as is the case for NarG and other MPT proteins. NapB is a *c*-type diheme protein. NapAB is well defined by the elucidation of the crystal structures from four different microbial species [82]. The catalytic molybdenum is coordinated by six sulfur atoms, four of which originate from the two dithiolene molybdopterin cofactors that both are present as tricyclic (pyranopterin) ring structures (Figure 8b). The *M. oxyfera* genes coding for NapAB (DAMO_2411 and DAMO_2410, respectively) form part of a larger gene cluster (DAMO_2408-2415) that includes the inventory for the nitrite reductase described next (Figure 9b). In DAMO_2411 and DAMO_2410, all amino acids implicated in NapAB crystal structures with the binding and structuring of the Mo-*bis*PGD, iron-sulfur and heme *c* cofactors are conserved. The identity suggests functionality of NapAB from *M. oyfera*, if expressed. In agreement with a periplasmic localization, DAMO-2410 contains a *tat* signal for protein export. Remarkably, the DAMO_2408-2415 cluster lacks any genes that in other Nap systems code for membrane-bound components, such as NapD, NapF, NapG, and NapH, that provide the electrons for nitrate reduction by the oxidation of menaquinol [84]. Since genes coding for such membrane-bound Nap components are absent in other parts of the genome as well, reduction of nitrate by *M. oxyfera* Nap might rely on a reduced cytochrome *c* pool.

The reduction of nitrite to NO in *M. oxyfera* is catalyzed by cytochrome cd_1 (NirS) of which structural and accessory genes are contained within the DAMO_2408-2415 cluster (Figure 9b). In this cluster, DAMO_2409 codes for a gene product comprising a fusion between a AsnC-family transcriptional regulator, and NirD/G and NirL/H involved in the biosynthesis of heme *d*. DAMO_2412 and DAMO_2413 code for two more heme *d* biosynthesis proteins, NirF and NirJ, respectively. The catalytic nitrite-reducing enzyme, NirS is derived from the DAMO_2415 gene. The DAMO_2415 amino acid sequence shows a remarkable high identity (61 %) to the one of *K. stuttgartiensis* NirS (kuste4136; see Section 3.1), but the *M. oxyfera* sequence is also highly similar to NirS from *Pseudomonas aeruginosa* NirS (53 % identity) and from *Paracoccus pantotrophus* NirS (53 % identity), both having known crystal structures [85]. Indeed, the identity encompasses the conservation in DAMO_2415 of all structurally and functionally relevant amino acids found in the crystal structures. In agreement with the central role in metabolism, DAMO_2415 is one of the highest expressed genes in the

genome and one of the most abundant proteins in the proteome [18]. Translated DAMO_2415 is preceded by an N-terminal signal sequence and antibodies raised against specific peptide sequences confirm its localization in the periplasm [86]. Protein translocation might be supported by the product of the DAMO_2408 gene in front of the DAMO_2408-2415 cluster (Figure 9b), which codes for YajC, one of the components of the Sec-YidC-YajC machinery for protein export and membrane protein insertion [87]. However, the DAMO_2408-2415 cluster again lacks one conspicuous candidate: The gene encoding NirC, a *c*-type cytochrome that provides the electron for nitrite reduction.

Besides the dissimilatory NirS, *M. oxyfera* contains the gene complement for an assimilatory nitrite reductase (NasBD). NasBD is composed of the NasD small subunit carrying a 2Fe2S Rieske-type iron-sulfur cluster and the NasB large subunit with a siroheme as its catalytic cofactor. The enzyme catalyzes the NAD(P)H-dependent reduction of nitrite to ammonium, similar to NrfA (see Section 3.4.2) [88]. In the genome of *M. oxyfera*, *nasB* (DAMO_0865; *nirB*) and *nasD* (DAMO_0864; *nirD*) belong to a larger gene cluster (DAMO_0859-0867) that covers a catalytic and regulatory inventory for nitrogen assimilation, such as NAD(P)H-dependent glutamine synthetase (GOGAT) and the NR_I-NR_{II} (*glnLG*; *ntrBC*) two-component regulatory system. However, genes coding for assimilatory nitrate reductase (NasAB) that are often found in *Nas* operons [89] are absent both in the DAMO_0859-0867 gene cluster as well as in other parts of the genome.

4.1.2 Nitric Oxide Reductase-like Proteins in *M. oxyfera*

Free radical nitric oxide is a highly reactive compound and nature has invented a plethora of enzymes that are capable to reduce NO to the less toxic N_2O (eq. 13). Denitrifying Bacteria and Archaea contain membrane-bound respiratory nitric oxide reductases (NOR). Interestingly, such NORs are also found in some non-denitrifying pathogenic bacteria, presumably to protect the cell against NO released by the host's immune system [90].

$$2\,NO + 2\,H^+ + 2\,\mathbf{e}^- \rightarrow H_2O + N_2O \quad (E_0{}' = +1.18\,V) \tag{13}$$

Initially two NOR subclasses were proposed based on amino acid sequences and type of electron donor [91], cytochrome *c*-dependent NOR (cNOR) that receives electrons from soluble protein electron donors (either cytochromes *c* or pseudoazurin) and quinol-dependent NOR (qNOR). Three-dimensional structures at atomic resolution were obtained for both types [92] and helped to establish the molecular details of this class of enzymes. An additional hybrid NOR, termed qCu_ANOR, has been described for *Bacillus azotoformans* that oxidizes both soluble cytochromes and membrane-embedded quinols [93]. The recent sequencing of the genome of *B. azotoformans* identified this qCu_ANOR as a sNOR [94], one of several novel NOR types [95] (see next). In the first genome survey of *M. oxyfera* three homologous nitric oxide reductase-encoding genes were detected, all three

proteins belonging to the group of qNORs. However, as outlined below two of these proteins likely have another function, whereas two more NORs can be added to the *M. oxyfera* repertoire due to erroneous annotation resulting from at least some confusion in the genomic NOR scenery.

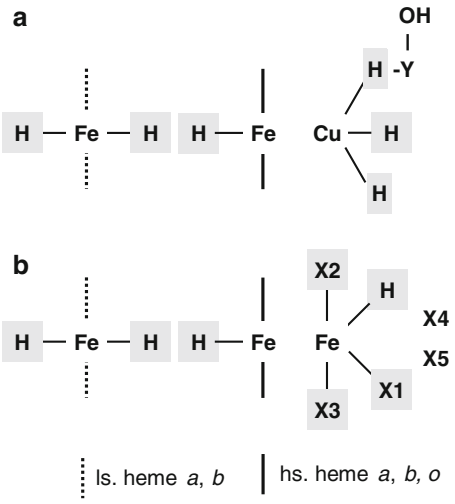

c

	X1	X2	X3	X4	X5
cNOR	H	H	E	E	E
qNOR	H	H	E	E	E
sNOR	H	H	N	Y	X
gNOR	D	H	D	L	E
NOD	H	N	Y	E	Q

Figure 10 Schematic representation of the catalytic site of members of the heme-copper oxidase superfamily represented by (**a**) oxidases and (**b**) dissimilatory nitric oxide reductases (NORs). The catalytic site comprises a low-spin (ls) heme for electron transfer and a binuclear catalytic part composed of a high-spin (hs) heme with either a copper ion (Cu_B) as in oxidases or an iron ion (Fe_B) as is the case with NORs. The different amino acids (H, X_1-X3) that coordinate these moieties are highlighted by light grey squares. X4 and X5 are second shell amino acids within the Fe_B coordination sphere at which the X5 (glutamate) in cytochrome *c*-dependent NOR (cNOR) has been implicated in proton transfer to the active site. X5 in sNORs is variable. (**c**) Amino acid variations (X1-X5) that are found in established and putative novel types of NORs are specified in the table.

Early sequence analyses [96] unambiguously identified NORs as members of the heme-copper oxidase (HCO) superfamily that comprises terminal oxidases such as the mitochondrial cytochrome *c* oxidase or the bacterial *cbb*$_3$ oxidase (see also Chapter 4). All members of the superfamily share sequence similarities in the catalytic subunit I. This subunit I is membrane-bound by 12 or 14 TMHs. In all known heme-copper oxidases, subunit I harbors a six-coordinated low-spin heme (*a* or *b*-type) that functions as electron mediator to the active site (Figure 10).

The active site, where substrate binds and is converted is a unique dinuclear center formed by a five-coordinated high-spin heme (*a*, *b* or *o*-type) and a non-heme metal. In oxygen-reducing HCO, the non-heme metal is a copper ion (Cu_B) able to cycle between Cu^+ and Cu^{2+}. All examined NORs harbor an iron ion at this position (Fe_B), which together with the heme-Fe forms a dinuclear iron site (Figure 10b), suitable to accommodate two NO molecules simultaneously and catalyze the reductive conversion to N_2O. Although it was found that the crystallized qNOR from *Geobacillus stearothermophilus* coordinated a zinc ion as the non-heme metal [92a] (Figure 11), it is regarded as an artifact based on the loss of catalytic activity when iron is substituted for zinc. How the type of metal contributes to the specific catalytic abilities resulting in NO or O_2 reduction is not understood. Interestingly in this respect is that some NO and O_2 reductases exhibit cross reactivity towards O_2 and NO, respectively [97].

The three metallic cofactors (two heme Fe and one Cu/Fe) in subunit I are ligated by six histidine residues (Figure 10). For a long time, these six histidines were thought to be invariant and diagnostic for all HCOs. Two histidines coordinate the electron-transferring low-spin heme iron, one histidine the active site high-spin heme iron and the remaining three are non-heme metal-coordinating. A crucial active-site residue, which is absent in NORs, is a conserved tyrosine that is covalently bound to one of the Cu_B-ligating histidines and acts as a temporary electron and proton donor during O_2 reduction [98]. This cross-linked tyrosine is critical to distinguish between NO- and O_2-reducing HCOs. In contrast, a characteristic feature for cNOR and qNOR enzymes is a conserved glutamate, which is part of the Fe_B ligation sphere providing a distorted trigonal bipyramidal coordination geometry to the iron ion. Yet, a detailed survey by Hemp and Gennis [95] of sequences that had been automatically annotated in Archaeal genomes as HCOs, highly suggests that the NOR picture is far from complete and more diffuse. For example, members of a family, referred to as sNORs [95], are phylogenetically closest related to O_2-reducing B-type oxidases and share a considerable sequence similarity to members of this subfamily. However, they lack the cross-linked tyrosine, and unlike cNORs and qNORs the Fe_B-ligating glutamate is substituted by an asparagine. The particular features are retrieved in the above-mentioned qCu_ANOR from *B. azotoformans* [94] and they are also found in HCO-like proteins from other denitrifying bacteria, including *M. oxyfera*.

4.1.3 The Making of Oxygen

As shown by genome analysis and activity experiments, O_2 is not only an essential but also a measureable intermediate in the nitrite-dependent anaerobic oxidation of methane in *M. oxyfera* [18]. Since external supply of oxygen was excluded, Ettwig et al. [18] postulated a mechanism by which NO serves as the source of intracellularly produced O_2. In the proposed scheme two molecules of NO are disproportionated into N_2 and O_2 (eq. 14).

$$2\ NO \rightarrow O_2 + N_2 \quad \left(\Delta G^{0\prime} = -173\,kJ \cdot mol^{-1} O_2\right) \tag{14}$$

This reaction is thermodynamically highly exergonic but kinetically challenging. The conversion of NO into O_2 and N_2 involves the breaking of two N-O double bonds together with the formation of an N-N triple bond and an O-O double bond and is thus assumed to proceed with low turnover rates. This chemistry has not been observed in biological systems before. Therefore, a candidate "nitric oxide dismutase" (NOD) that could catalyze this reaction could not be identified by homology.

Besides the primary question, which enzyme would catalyze NO dismutation, even puzzling was that the genome of *M. oxyfera* coded for three qNOR homologs [18]. Two of these (DAMO_2437 and DAMO_2434) were among the most abundantly expressed proteins; the third one (DAMO_1889) was hardly expressed. The presence in the genome and expressions of these qNOR-like proteins opposed the observation that the microorganism produced N_2O at trace levels only, while the gene coding for the only known enzyme capable of N_2O reduction, N_2OR, could not be detected. Furthermore, the detailed inspection of the DAMO_2437 and DAMO_2434 sequences exhibited amino acid substitutions at positions that were recognized in canonical qNOR as being essential for electron transfer and reductive conversion of NO [99].

Crystallization of the *Geobacillus stearothermophilus* qNOR in the presence of the quinol analogue 2-heptyl hydroxyquinoline N-oxide (HQNO) permitted the identification of a specific binding site for (mena)quinol (Figure 11b) [92a]. Part of this binding pocket is provided by several semi-conserved hydrophobic residues that form a binding groove for the hydrocarbon tail of the quinol moiety. Specific interactions with functional groups of the HQNO core are formed by a set of highly conserved amino acids. His328 and Asp746 (*Geobacillus* numbering) form H-bonds with the NO and OH groups, respectively. In DAMO_2437 and DAMO_2434 both of these residues are substituted mostly by functionally dissimilar amino acids (Figure 11c) and it is thus conceivable that quinol binding and consequently electron donation is impaired in these proteins. Since alternative electron entry sites are absent (cytochrome *c* as in cNOR and Cu_A as in sNOR) in DAMO_2437 and DAMO_2434, electron-consuming NO conversion seems unlikely. Additional features of DAMO_2437 and DAMO_2434 are a slightly altered active site configuration (Figure 11e). One of the three Fe_B coordinating His residues (His560 DAMO_2437 numbering) is exchanged for an asparagine. Next, the highly conserved second coordination shell Glu581, which was implicated in proton transfer to the active site in cNOR [100] is replaced by a glutamine. Although variations in the amino acid composition of the catalytic site in NOR seem to be more widespread than anticipated, the particular deviations observed in DAMO_2437 and DAMO_2434 clearly disfavor a role as NOR. The deviations very well might facilitate another reaction, NO disproportionation.

Importantly, the specific substitutions are conserved in some other proteins in genome databases, namely close homologs of DAMO_2437 and DAMO_2434 in

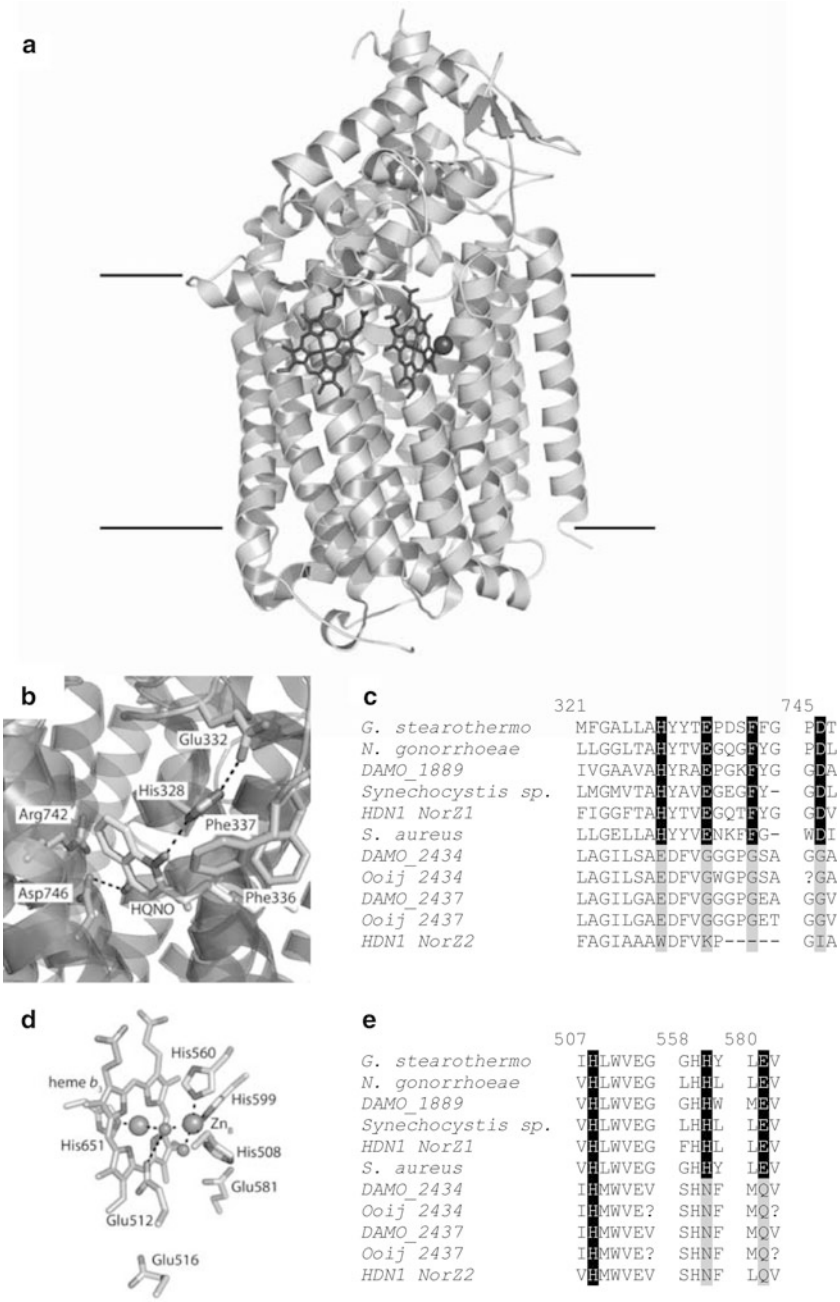

Figure 11 Overall structure of quinol-dependent nitric oxide reductase (qNOR) from *Geobacillus stearothermophilus* (**a**), its quinol-binding site (**b**) and active site configuration (**d**). Specific differences in quinol-binding (**c**) and catalytic sites (**e**) between qNORs and putative NO dismutases (NOD) are highlighted in the multiple amino acid sequence alignments. (**a**) Ribbon representation of the qNOR overall structure and the position of the active site. Horizontal lines bound the membrane lipid bilayer. (**b**) Quinol binding site harboring the quinol analog 2-heptyl

the NC10 enrichment culture strain Ooij and a putative NOR from the γ proteobacterial strain HdN1 (Figures 11c and e) [99]. HdN1 is capable of growth on C6-C20 alkanes [101]. Growth on hexadecane proceeds with oxygen, nitrate or nitrite as electron acceptors but not with N_2O. However, N_2O does serve as the oxidant with hexadecanol or hexadecanoic acid as substrates, compounds that do not require the oxidative activation of a C-H bond. Even though the genome of HdN1 lacks any genes coding for the glycyl-radical-catalyzed activation of alkanes, two or three monooxygenase-encoding genes are present. Taken together, these observations suggest that alkane activation in HdN1 and methane activation in *M. oxyfera* might proceed in similar ways, supported by oxygen that is made via nitrate and nitrite by a NOR-like NO dismutase.

4.1.4 Nitric Oxide and Oxygen Reduction

Unlike DAMO_2437 and DAMO_2434, the amino acid sequence of DAMO_1889 complies with a functional qNOR (Figures 11c and e). As already mentioned, the gene is hardly expressed, which accords the insignificant N_2O production in *M. oxyfera* cultures growing on methane and nitrite [18]. Nevertheless, the situation regarding NO reduction could be more complicated at the genomic and physiological levels.

The nitrite-dependent conversion of methane (eq. 3) is associated with a theoretical surplus of one molecule of O_2 and four electrons. Whole cells are capable of O_2 reduction at rates that exceed the methane-converting metabolic activity [29]. Indeed, the genome of *M. oxyfera* seemed to harbor no less than three different HCO-type oxidases, next to a plant-like alternative oxidase [18, 29]. Supported by substrate-specific O_2 reduction rates and expression data, it was argued [29] that the residual O_2 would be reduced to water by DAMO_1118-19. This protein complex had been annotated as a bo_3-type oxidase belonging to the class A2 of heme-copper oxidases. A reevaluation now of the protein sequence reveals that DAMO_1118-19 is not an O_2 reductase but rather a member of a divergent type of gNORs. Similarly, DAMO_0801-02, which was being annotated as ba_3 oxidase, appears to belong to

Figure 11 (continued) hydroxyquinoline *N*-oxide (HQNO). The Zn atom seen in (**d**) most likely represents a crystallization artifact and would be replaced by an Fe atom in the catalytically active enzyme. qNORS from different microbial species with protein identifiers in parentheses are the following: *G. stearothermo, G. stearothermophilus* (3YAG); *N. gonorrhoeae*, *Neisseria gonorrhoeae* 1291(EEH62456); DAMO_1889, qNOR from *Methylomirabilis oxyfera*; *Synochocystis* sp. (BAA18795); HDN1 NorZ1, γ Proteobacterium strain HDN1 (CBL45628); *S. aureus*, *Staphylococcus aureus* (EGL94648). Putative NODs: DAMO_2434, Ooij 2434, DAMO_2437, Ooij 2437, proteins from the *M. oxyfera* enrichment cultures "Twente" (DAMO) and "Ooij" [18]; HDN1 NorZ2 (CBL43845). Structural figures (PDB ID: 3AYG; [92a]) were prepared in PyMOL [48].

the new NO-reductase type of sNORs. The only oxidase that stands a proper annotation, namely as an aa_3-type oxidase, is DAMO_1162-65. The aa_3-type oxidase, which is the most efficient proton-pumping terminal oxidase but which has an only low affinity for oxygen, tends to be expressed under high-oxygen conditions. A role of the DAMO_1162-65 aa_3-type oxidase as being responsible for O_2 reduction could be ruled out on the basis of too low activities and too low expression values indeed [29]. Hence, it is still an open issue, which enzyme from *M. oxyfera* acts in O_2 removal. Considering that oxygen reductase activity with turnover numbers up to 8.4 μmol $O_2 \cdot min^{-1} \cdot mg^{-1}$ protein has been demonstrated for c- and qNOR [97, 102], one of the NO reductases, perhaps even gNOR DAMO_1118-19, might moonlight as an O_2 reductase. And taking the slow metabolic rates of *M. oxyfera* (1–2 nmol $CH_4 \cdot min^{-1} \cdot mg^{-1}$ protein) into account, an even minute amount of NOR would sustain oxygen reduction.

However lowly expressed under standard growth, the question remains what the redundant set of known qNOR (DAMO_1889), and new gNOR (DAMO_1118-19) and sNOR (DAMO_0801-02) would do. The set may provide the organism with a means to cope with nitrosative stress invoked by other members of a denitrifying community. Next, NO is an essential intermediary substrate of nitrite-dependent methane oxidation and the tight balancing of its production and subsequent (quite slow) conversion is necessary to avoid harmful concentrations. The balance could be easily disturbed by the uptake of external electron donors more oxidized than methane, such as formate, immediately resulting in excess nitrite reduction to NO. Under such conditions, reductive conversion of NO into N_2O is advantageous over its disproportionation into N_2 and O_2, which is expected to occur very slowly thereby requiring a vast amount of enzyme for appreciable activity.

4.2 The Methane Oxidation Pathway

4.2.1 The Activation of Methane into Methanol

In aerobic methanotrophs, inert methane is activated to methanol by the insertion of an oxygen atom from O_2. The other oxygen atom is reduced to water (eq. 15). Methane activation is catalyzed by two different methane monooxygenases (MMO), a particulate, membrane-bound (pMMO) and a soluble (sMMO) form. *M. oxyfera* contains only pMMO. Although the enzyme has already been discussed in detail in Chapter 6 of this Volume, we will recall some of its main structural properties for the sake of comparison.

$$CH_4 + O_2 + 2\ H^+ + 2\ \mathbf{e}^- \rightarrow CH_3OH + 2\ H_2O \quad (E_0' = +1.46\,V) \qquad (15)$$

Supported by the resolution of the crystal structures from three different methanotrophs [103], the common view is that pMMO is composed of $\alpha_3\beta_3\gamma_3$ trimers with three copies each of the pmoA, pmoB, and pmoC subunits ordered

in a cylindrical way within the cell membrane. PmoA is primarily composed of 6–7 TMHs; three conserved periplasmic aromatic amino acids (F50, W51, W54; numbering according to the *Methylococcus capsulatus* structure) are proposed to line a methane substrate channel [2]. Also pmoC is membrane-bound by 5 TMHs. PmoB is structured by two cupredoxin domains located in the N-and C-terminal parts. Both domains are separated by two TMHs, but they are positioned next to each other by a linker loop; a third TMH is N-terminally cleaved. The cupredoxin domains face the periplasm and represent the only soluble part of the enzyme complex. Sandwiched between the two cupredoxin domains, three histidines (H33, H137, H139) ligate a dicopper center in the *M. capsulatus* protein [103], but the *Methylocystis* structure is more ambiguous, showing both one and two copper atoms at this side [103]. By stripping the two THMs from pmoB and connecting the cupredoxin domains by a short linker such that the overall structure was maintained, a copper-containing recombinant protein was made that was catalytically active by itself, both with methane and the abiological substrate propylene [104]. This clever approach clearly shows that pmoB is the catalytic site. Also the other subunits may bind copper and/or zinc atoms, but there is at least some disagreement concerning the relevance of these metals; they could have been the artificial result of enzyme purification and crystallization methods [2].

The genome of *M. oxyfera* harbors one pMMO, the subunits of which are encoded by DAMO_2451 (*pmoC1*), DAMO_2450 (*pmoA*), and DAMO_2448 (*pmoB*). Consistent with their central role in metabolism, the three genes are among the highest expressed, both at the transcriptome and proteome levels [18]. Immunogold labeling of affinity-purified antibodies raised against the soluble part of pmoB localize it at the periplasmic side of the cell membrane as expected [86]. DAMO_2339 codes for a second *pmoC*, which is identical to DAMO_2451. Downstream of DAMO_2448, DAMO_2446 has been annotated as pmoD1 of which a second copy (pmoD2; 84 % sequence identity) is found as DAMO_2340. PmoD is predicted to be an exported protein that remains membrane-bound by one TMH in the C-terminus. Homologs of this protein are found in genomes of many methanotrophic and non-methanotrophic species. Contrary to *M. oxyfera*, those *pmoD* homologs are never linked to genes encoding pMMOs and it is questionable whether pmoD forms part of the pMMO complex in *M. oxyfera*. At first sight, sequence identities of pmoA, pmoB, and pmoC from *M. oxyfera* are not very high (~50 %) with respect to the ones in pMMOs with known crystal structures and phylogenetic analyses place all three *M. oxyfera* subunits in a separate clade [18]. Nevertheless, subunit sequences of verified pMMOs are also quite divergent. In fact, a closer comparison reveals the complete conservation in *M. oxyfera* pMMO of all secondary structural elements (TMHs and their topology, β barrel strands in the cupredoxin domains) with respect to those with known crystal structures. Moreover, all amino acids that have been implicated in the binding of metals, no matter their eventual biochemical relevance, are present in pmoA, pmoB, and pmoC from *M. oxyfera*. These similarities suggest a same overall architecture of *M. oxyfera* pMMO and a same function, namely the oxygen-dependent activation of methane (eq. 15). In agreement herewith, in experiments

with whole cells the role of oxygen was substantiated in propylene epoxidation, a widely applied artificial reaction to follow pMMO activity [18].

$$CH_4 + NO \rightarrow CH_3OH + 0.5\ N_2 \quad \left(\Delta G^{0\prime} = -211\,\text{kJ}\cdot\text{reaction}^{-1}\right) \tag{16}$$

$$CH_4 + N_2O \rightarrow CH_3OH + N_2 \quad \left(\Delta G^{0\prime} = -223\,\text{kJ}\cdot\text{reaction}^{-1}\right) \tag{17}$$

Structural considerations and the observed role for oxygen in propylene epoxidation do not preclude an alternative view for methane activation by *M. oxyfera*, namely by using the oxidative power of NO (or N_2O) (eqs 16 and 17). Although thermodynamically highly feasible, the reactions are incompatible with the physiology of *M. oxyfera*. Apart from the mechanistic problem how dinitrogen gas would be produced in case of activation by one NO, it can be inferred that substantial amounts of N_2O should be formed to maintain the redox balance. Since no electrons are required for methane activation (Figure 2), the only way to get rid of the extra electrons would be nitrite reduction to the level of N_2O. In active metabolizing cells, the gas can only be detected at trace levels [18].

4.2.2 Methanol Oxidation

Microorganisms have two different types of enzymes at their disposal to oxidize methanol, the product of methane activation. Gram-positive bacteria utilize methanol dehydrogenases that take $NAD(P)^+$ as the electron acceptor and that are localized in the cytoplasm [105]. In Gram-negative methylo- or methanotrophs, a periplasmic MDH is present, which belongs to the broad class of pyrroloquinoline quinone (PQQ)-containing proteins (quinoproteins) [106]. The particular quinoproteins are structured by eight sets of four-stranded, antiparallel W-shaped β sheets that tightly pack the protein backbone into eight propeller-like peptide sequences according to a pseudo eight-fold symmetry axis (Figure 12). The catalytic cofactor, PQQ, is located central to the propellers, buried deeply inside a hydrophobic pocket. PQQ is kept in position by a series of in-plane hydrogen bonds to the side chains and carbonyl groups of a conserved set of amino acids.

Different types of quinoproteins catalyze the oxidation of a wide range of alcohol and aldehyde substrates and each type is more or less tuned for a specific substrate. The oxidation occurs at the PQQ cofactor and involves a base-catalyzed proton abstraction in concert with the transfer of a hydride from the substrate to PQQ (Figure 13) [107]. By accepting the hydride, PQQ gets reduced to $PQQH_2$. After the subsequent transfer of two electrons to an associated electron carrier, a *c*-type heme protein, $PQQH_2$ is re-oxidized and the enzyme is prepared for a next reaction cycle. In most quinoproteins studied to date, a calcium ion in close vicinity to PQQ assists in hydride abstraction. By acting as a Lewis-acid, the C5-O5 bond in PQQ is polarized, which facilitates the nucleophilic addition of the hydride to C5 (Figure 13). The Ca^{2+} ion is kept in the right configuration by the coordination to two highly conserved amino acids, a glutamate and an asparagine (Figures 12c and d). Proton abstraction is assisted by a conserved aspartate.

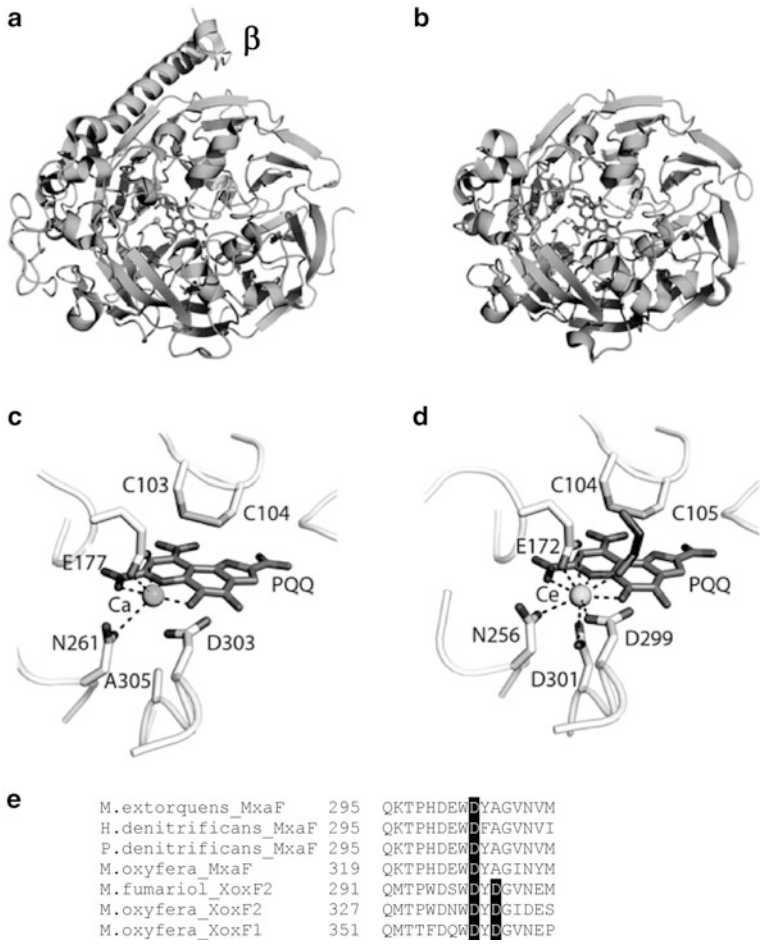

Figure 12 Structures of MxaFI- and XoxF-type methanol dehydrogenases (MDH). A bottom view of the MxaFI-type MDH from *Methylobacterium extorquens* AM1 (PDB ID: 1W6S; [109 g]) composed of the large (MxaF) subunit with the PQQ catalytic site in the center and its small (MxaI, β subunit) is shown in panel (**a**). Panel (**c**) presents a detailed view of the catalytic site in which a Ca ion is coordinated by PQQ. A bottom view of the XoxF-type MDH from *Methylacidiphilum fumariolicum* SolV (PDB ID: 4MAE) [114] and details of its catalytic site are presented in panels (**b**) and (**d**), respectively. Note that PQQ now is associated with a Ce ion that is additionally coordinated by an aspartate (D301). This aspartate residue is also present in two XoxF-MDHs from *Methylomirabilis oxyfera* (**e**). In the sequence alignment (**e**), proteins with their (protein) database identifiers in parentheses are the following: M.extorquens_MxaF (1 W61); H.denitrificans_MxaF (2D0V); P.denitrificans_MxaF (1LRW); M.oxyfera_MxaF (DAMO_0112); M.fumariol_XoxF2 (4MAE); M.oxyfera_XoxF1 (DAMO_0124); M.oxyfera_XoxF2 (DAMO_0134). Structural figures were prepared by PyMOL [48].

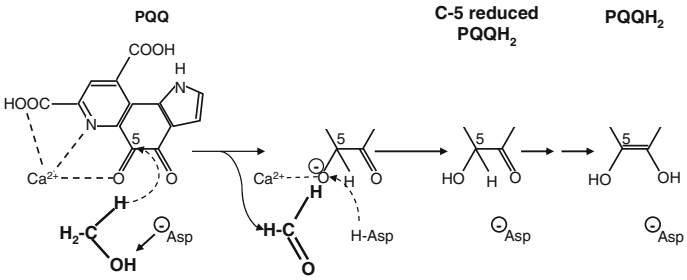

Figure 13 Catalytic mechanism of PQQ-dependent methanol dehydrogenase. The scheme was adapted from [108].

$$CH_3OH \rightarrow HCHO + 2\ H^+ + 2\ \mathbf{e}^- \quad (E_0' = -0.182\,V) \tag{18}$$

MDH catalyzes the oxidation of methanol to formaldehyde according to equation (18). The genome of *M. oxyfera* codes for three MDH quinoprotein systems (MDH1-3) that are uniquely located on one large cluster (DAMO_0112-0138) (Figure 14). In the MDH1 system (DAMO_0112-122), DAMO_0112 (*mxaF*) and DAMO_0115 (*mxaI*) encode the large (α) and small (β) subunits, respectively, of the canonical heterodimeric ($\alpha_2\beta_2$) MxaFI-type of MDH. This type of MDH that carries calcium as a PQQ-associated metal cofactor is well understood by the resolution of the crystal structures from seven different microbial species [109]. Besides these structural genes, the MDH1 system comprises a range of other genes that are commonly associated with the functionality of MxaFI-MDH and that are ordered as also seen in *M. oxyfera* [110]. DAMO_0114 codes for the cognate electron carrier, cytochrome c_L (MxaG) and DAMO_0113 for a periplasmic solute-binding protein (MxaJ) with an as-yet unknown function. DAMO_0116-0121 find their homologs (MxaRSACKLD) for instance in *Methylobacterium extorquens*, a methylotrophic model organism, where these gene products have been implemented with Ca^{2+} insertion [110]. In the latter organism, MxaE (DAMO_0122 in *M. oxyfera*) is additionally required for MxaFI maturation. Quite astonishingly, *M. oxyfera* lacks the gene inventory (*pqqABCDEF*) [111] for PQQ biosynthesis [112]. This would make the organism dependent on other microorganisms in its environment that supply *M. oxyfera* with a crucial cofactor of one of its key enzymes.

The MDH2 and MDH3 systems code for divergent types of MDH quinoproteins, termed XoxF-MDHs, which display sequence identities of less than 50 % with MxaF large subunits. XoxF proteins are widely found in genomes of methylotrophs and methanotrophs, but also in genomes of organisms that are as yet unknown for such lifestyles. Their function has been enigmatic for quite some time [19]. The recent purification and characterization of XoxF proteins from different species [113], and the elucidation of the atomic structure of one of these [114] solved the enigma. Just like MxaFI-MDH, XoxF is a methanol-oxidizing quinoprotein. In fact, large subunit structures are fully superimposable (Figures 12a and b). However,

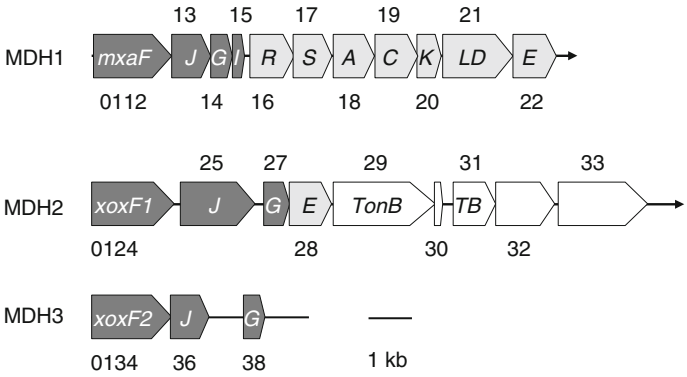

Figure 14 Genomic organization of three methanol dehydrogenase (MDH) systems within the DAMO_0112-038 gene cluster from *Methylomirabilis oxyfera*. Structural genes are shaded dark grey with white lettering and accessory genes are in light grey. Gene lengths and intergenic regions are drawn to scale. TonB, TB, TonB-dependent uptake system.

there are two major differences: XoxF-MDH is a homodimeric protein (α_2) composed of a large PQQ-containing subunit only and PQQ is associated with a rare earth element (REE) instead of Ca^{2+} (Figure 12d). REEs, such as cerium or lanthanum, are stronger Lewis acids, lending XoxF-MDHs a catalytic efficiency that is superior to their MxaFI-MDH counterparts [114, 115]. Because radii of REE ions are bigger than of Ca^{2+}, their proper accommodation requires a specific adaptation of the amino acid sequence. This adaptation is found in a specific aspartate residue that provides an additional ligand and that is located two positions downstream of the catalytic aspartate (Figure 12e) [114, 115].

The various features can be discerned in the further inspection of the MDH2 (DAMO_0124-0133) and MDH3 (DAMO_0134-0138) gene systems from *M. oxyfera* (Figure 14). Herein, DAMO_0124 and DAMO_0134 code for XoxF large subunit homologs [116]. Their amino acid sequences show the conservation of the catalytic aspartate and of the amino acids involved in PQQ and metal association, including the aspartate related with REE coordination (Figure 12e). Still, DAMO_0124 and DAMO_0134 share only 43 % sequence identity and phylogenetic analysis addresses these proteins to two different types of XoxF-MDHs, namely XoxF1 and XoxF2, respectively. (One may note that no less than five types of XoxF proteins can be distinguished [19]). The MDH1 and MDH2 systems lack genes that code for small subunits, but genes encoding cytochrome c_L (*xoxG*) and *xoxJ* paralogs are present (Figure 14). Next, the MDH2 and MDH3 sub-clusters lack any genes involved in Ca^{2+} insertion, which is common in XoxF systems [115]. Quite unusually, the MDH2 sub-cluster harbors a second *mxaE* copy. Two genes in the latter sub-cluster code for TonB-dependent uptake proteins. These uptake proteins are consistently detected in genomes of microorganisms that contain XoxF-type MDHs and they might play a role in the acquirement of poorly soluble REEs [115].

The straightforward question is which of the three MDHs is functionally expressed in *M. oxyfera*. The answer is somewhat surprising. The only methanol-oxidizing enzyme that could be isolated was a heterodimer ($\alpha_2\beta_2$) composed of XoxF1 (DAMO_0124) large subunits and MxaI (DAMO_0115) small subunits [116]. Although the diagnostic REE-binding aspartate is apparent in the DAMO_0124 amino acid sequence, it is unknown whether the protein does harbor a REE indeed. It is conceivable that in the presence of more available Ca^{2+} the latter atom is bound, its coordination being assisted by the small subunit. Such assistance would allocate the subunit a function.

4.2.3 Formaldehyde Oxidation

Out of the many ways to oxidize formaldehyde biochemically, *M. oxyfera* potentially uses two (Figure 15). In the first pathway, 5,6,7,8-tetrahydromethanopterin (H_4MPT) acts as the one-carbon unit (C1) carrier. Enzymes of this pathway are highest expressed at the transcriptional and protein levels [18] indicating that major part of the formaldehyde flux passes this branch. The second, only lowly expressed pathway is an analogous one with 5,6,7,8-tetrahydrofolate (H_4F) as C1-carrier serving biosynthetic reactions (Figure 15c).

The H_4MPT-dependent pathway is found in many methylo- and methanotrophs [19], and also in methylotrophic methanogens. Hydrogenotrophic methanogens that produce methane by the reduction of CO_2 or by the disproportionation of formate use the route in the reversed order (see Chapter 6 of ref. [138]). In *M. oxyfera*, all enzymes of the H_4MPT pathway are encoded on a large gene cluster (DAMO_0454-0473) (Figure 15a) highly resembling the organization in methylotrophs [117]. Besides H_4MPT-dependent metabolic enzymes, the *M. oxyfera* cluster comprises genes that encode one of three formate/formyl oxidation systems described hereafter (see Section 4.2.4) as well as a conserved set of genes that have been implicated in H_4MPT biosynthesis [117]. Next, the DAMO_0454-0473 cluster comprises various conserved genes that are absent in methylotrophic C1-transfer clusters, possibly involved in the as-yet elusive synthesis of the second C1-carrier in the route, methanofuran (MFR).

In the H_4MPT route, formaldehyde oxidation starts with the binding of the substrate to the C1 carrier to make 5,10-methylene- H_4MPT (Figure 15b). This reaction is catalyzed by the formaldehyde activating enzyme (Fae). 5,10-methylene-H_4MPT oxidation by methylene-H_4MPT dehydrogenase (Mtd) generates 5,10-methenyl-H_4MPT, which is converted to 5-formyl-H_4MPT by methenyl-H_4MPT cyclohydrolase (Mch). Fae (DAMO_0454) from *M. oxyfera* displays 58 % sequence identity to Fae from *M. extorquens* [118] and Mch (DAMO_0461) is 40–44 % identical to Mch enzymes from different sources with known crystal structures ([119]; PDB ID: 4FIO). In agreement with the anticipated function, sequence identities include the presence of critical amino acids for the binding of substrates and for catalysis. However, the role of the Mtd protein (DAMO_0455) could be more ambiguous. Whereas Mtd proteins from

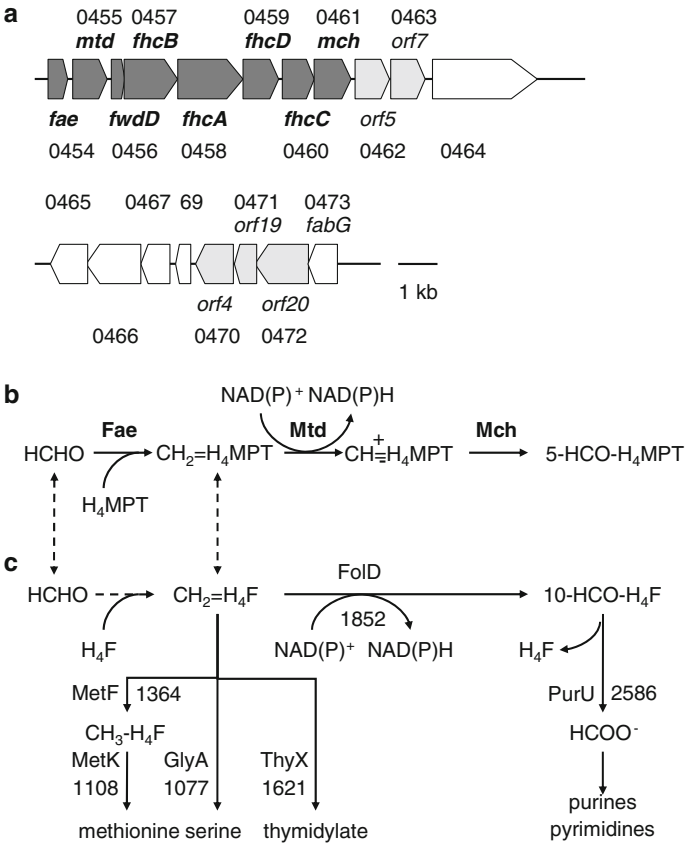

Figure 15 Tetrahydromethanopterin (H_4MPT)- and tetrahydrofolate (H_4F)-dependent formaldehyde and formate conversion systems in *Methylomirabilis oxyfera*. (**a**) Gene arrangement of the H_4MPT-dependent route on the DAMO_0454-0473 gene cluster. Gene lengths and intergenic regions are drawn to scale. Structural genes are shaded dark grey. A conserved set of genes also found in genomes of other methylotrophs that are suggested to be involved in the biosynthesis of H_4MPT [117] is shaded light grey. Herein, *orf5* codes for an α-L-glutamate ligase (RimK family), *orf7* for an ATP: dephospho-CoA triphosphoribosyl transferase (CitG), *orf4* for β-ribofuranosylaminobenzene 5′-phosphate synthase, *orf19* for a conserved protein (DUF447), and orf20 for a dihydropteroate synthase-related protein; FabG, 3-oxoacyl-(acyl-carrier protein) reductase. Other abbreviations are as specified in the text. (**b**) Pathway of H_4MPT-dependent formaldehyde oxidation. (**c**) Pathway of formaldehyde conversion to formate and its linkage with biosynthetic reactions using H_4F as the C1 carrier. Protein codes are indicated together with protein identifiers (DAMO_). The connection between H_4MPT (b)- and H_4F (c)-dependent pathways is indicated by dashed lines.

methanogenic and sulfate-reducing Archaea that use coenzyme F_{420} as electron acceptor are already quite divergent from $NAD(P)^+$-dependent Mtd proteins from methylotrophs, the latter also distribute in no less than five different phylogenetic clades (MtdA-E) [19]. These Mtd types markedly differ in substrate affinities.

The MtdB enzyme is specific for 5,10-methylene-H_4MPT in combination with both NAD^+ for energy generation and $NADP^+$ for biosynthesis [120]. The MtdA protein exclusively relies on $NADP^+$ but it can use 5,10-methylene-H_4MPT and 5,10-methylene-H_4F to variable degrees [121]. MtdC proteins are even more promiscuous in these respects [122]. The Mtd from *M. oxyfera* takes a unique intermediary position in between the MtdB and MtdA clades [19]. The sequence comparison between the *M. oxyfera* protein and MtdA from *M. extorquens* having a known crystal structure [123] reveals the nearly complete conservation of $NADP^+$-binding amino acids, but amino acids in the H_4MPT/H_4F-binding domain in *M. extorquens* MtdA are less well conserved in the *M. oxyfera* protein sequence. Apparently, *M. oxyfera* Mtd evolved such as to optimally sustain catabolism, i.e., substrate oxidation to CO_2, and C1 anabolism through H_4F-dependent reactions (Figures 15b and c).

The H_4F-dependent counterpart in between the formaldehyde and formate oxidation states is the bifunctional $NAD(P)^+$-dependent 5,10-methylene-H_4F:5,10-methenyl-H_4F cyclohydrolase (FolD, DAMO_1852) that generates 10-formyl-H_4F (Figure 15c). Substrates might be supplied to this enzyme in connection with Mtd activity just described or by the non-enzymic binding of formaldehyde to H_4F generating 5,10-methylene-H_4F. The various H_4folate derivatives are substrates for amino acid (serine, methionine) and purine (thymidylate) syntheses that depend on C1 compounds. In *M. oxyfera*, all enzymes involved use H_4F as the C1 carrier, underlining the central role of this cofactor in biosynthetic processes. Formate for purine synthesis can be formed by 10-formyl-H_4F lyase (PurU, DAMO_2586) that hydrolyzes 10-formyl-H_4F into formate and H_4F. However, there may be more means to make formate.

4.2.4 Formate Oxidation

Formate is a powerful electron donor that plays a key role in the energy metabolism of many respiratory and fermentative microorganisms. Nature has evolved an amazing variation in the way formate is oxidized to CO_2 by formate dehydrogenases (eq. 19), first and for all regarding their structural and functional organization [124]. The common property is the presence of a pterin cofactor (*bis*PGD) in the catalytic FDH subunit [125]. In FDHs, the cofactor is coordinated to either molybdenum (Mo-*bis*PGD) or tungsten (W-*bis*PGD) at which the metal additionally binds either cysteine or selenocysteine.

$$HCOO^- + H^+ \rightarrow CO_2 + 2\ H^+ + 2\ \mathbf{e}^- \qquad (E_0' = -0.44\,V) \qquad (19)$$

$$\text{formyl-MFR} + H_2O \rightarrow CO_2 + 2\ H^+ + 2\ \mathbf{e}^- + \text{MFR} \qquad (E_0' = -0.51\,V) \qquad (20)$$

$$\text{5-formyl-}H_4\text{MPT} + \text{MFR} \rightarrow H_4\text{MPT} + \text{formyl-MFR} \qquad \left(\Delta G^{0\prime} = -5\,\text{kJ}\cdot\text{reaction}^{-1}\right) \qquad (21)$$

$$\text{formyl-MFR} + H_2O \rightarrow \text{MFR} + HCOO^- \quad \left(\Delta G^{0\prime} = -15\,\text{kJ}\cdot\text{reaction}^{-1}\right) \quad (22)$$

In methanogenic and sulfate-reducing Archaea, the formyl group bound to methanofuran is oxidized to CO_2 by formyl-MFR dehydrogenase (fMFR-DH) (eq. 20; see also Chapter 6 of ref. [138]). As is the case with FDHs, the catalytic subunit is a MPT protein carrying either molybdenum (Fmd systems) or tungsten (Fwd systems) [126]. Again, these metals are coordinated to either cysteine or selenocysteine.

M. oxyfera has the disposal of three different formate/formyl oxidation systems (Figure 16). The first one (FwdDFhcBADC; DAMO_0456-0460) is coded as part of the formaldehyde-oxidizing gene cluster (DAMO_0454-0473) (Figure 15). Herein, *M. oxyfera* FhcBADC resembles the four-subunit formyl transferase/hydrolase (Fhc) from aerobic methylotrophs that is associated in these organisms with the C1 cluster as well [127]. Indeed, *M. oxyfera* FhcD (DAMO_0459) shows 48 % sequence identity to FhcD from *M. extorquens* that has been identified as 5-formyl-H_4MPT: methanofuran formyltransferase catalyzing reaction (21) [128]. In methanogenic and sulfate-reducing Archaea, this formyltransferase is present as a separate enzyme. Remarkably, the sequence identity of DAMO_0459 is even higher (53 %) with the formyltransferase from the distantly related methanogen *Methanopyrus kandleri*, having a known crystal structure [129], than with *M. extorquens* FhcD. *M. oxyfera* FhcA (DAMO_0458) is homologous both to *M. extorquens* FhcA and to the FwdA subunit of archaeal Fwd systems. This polypeptide is a member of the superfamily of metallo-dependent amidohydrolases and likely catalyzes formyl-MFR hydrolysis to formate (eq. 22). Formation of formate by the *M. extorquens* FhcCDAB complex is consistent with such a role [127]. *M. oxyfera* FhcC (DAMO_0460) has its homologs in FhcC from methylotrophs and in archaeal FwdC/FmdC subunits. FhcB from *M. oxyfera* (DAMO_0457) is an interesting case.

While the sequence identity with FhcB from *M. extorquens* is only low (22 %), the identity with cysteine- or selenocysteine-containing FwdB subunits [130] is much higher, especially with respect to *M. kandleri* (~46 %). In Archaea, FwdB mostly represents the MPT-catalytic subunit [130, 131]. FhcB from *M. oxyfera* shares with the *M. kandleri* FwdB subunits (MK0259 and MK1527) the presence in the N-terminus of four cysteines that commonly coordinate the 4Fe4S cluster in MPT catalytic subunits. Next, three cysteines are conserved in DAMO_0457 with respect to MK0259, two of which are substituted in MK1527 by a selenocysteine and a serine. These similarities highly suggest a role of the DAMO_0456-0460 system as a formyltransferase/cysteine-containing formylmethanofuran dehydrogenase. In agreement with the proposal, DAMO_0456-0460 possesses one more component, FwdD (DAMO_0456), which is unique for a non-Archaeon. Thus far, the FwdD subunit has only been found in archaeal tungsten- or molybdenum-containing (here: FmdE) fMFR-DHs. *M. extorquens* FhcB lacks the afore-mentioned cysteines and the Fhc complex is devoid of an FwdD-like subunit [127]. These differences would make the complex from aerobic methylotrophs inactive in formyl oxidation, restricting its function to a formyltransferase/formate-generating hydrolase [127]. Irrespective of its novelty, the FwdDFhcBADC system from *M. oxyfera* leaves

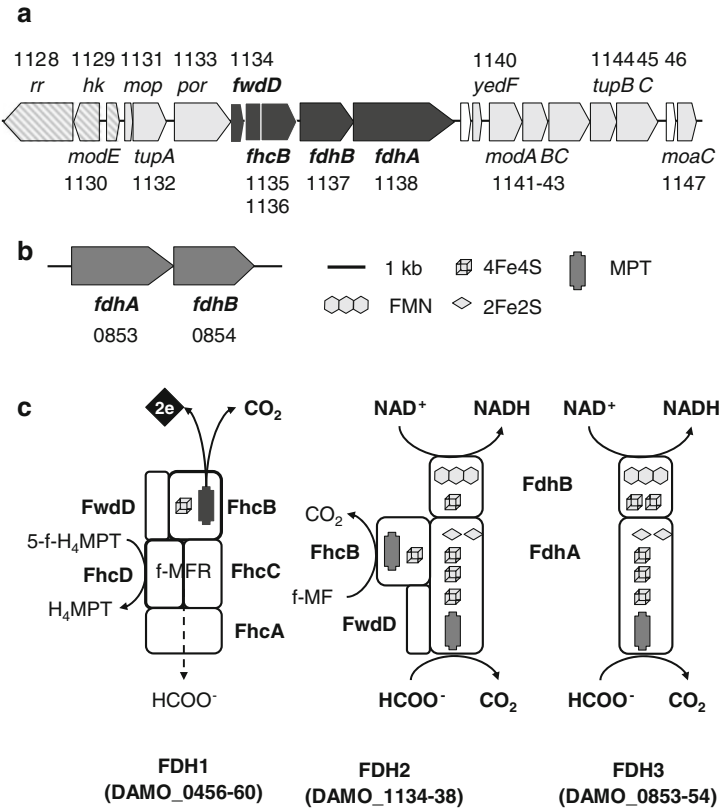

Figure 16 Three formyl/formate dehydrogenase (FDH) systems in *Methylomirabilis oxyfera*. The gene cluster organization of FDH 2 (DAMO_1128-1148) and FDH3 (DAMO_0853-0854) are shown in panels (**a**) and (**b**), respectively. Gene lengths and intergenic regions are drawn to scale. Structural genes are shaded dark grey and accessory genes are in light grey. Regulatory genes are hatched in diagonals. Genes coding for FDH1 form part of the H_4MPT-dependent formaldehyde oxidation gene cluster shown in Figure 15a. Panel (**c**) illustrates a model for the functional organization of FDHI, FDH2, and FHD3. Structural motifs are specified in the figure. Abbreviations and further explanations: rr, response regulator; hk, histidine kinase; modE, molybdenum uptake regulator; modABC, molybdenum uptake system; tupABC, tungsten uptake system; mop, molybdenum-pterin binding protein; por, porin; yedF, selenium metabolism protein; moaC, molybdopterin biosynthesis protein; MPT, *bis*(pyrano guanine dinucleotide); f-MFR, formylmethanofuran.

us with one issue: Where do the electrons from formyl/formate oxidation (eq. 20) go to? All components are predicted to be cytoplasmic soluble proteins and the encoding genes are not linked to ones (FwdFG) that code for iron-sulfur electron transfer proteins in archaeal Fwd systems [130, 131]. Unfortunately, the genome of *M. oxyfera* does not give an immediate clue to the issue.

Next to the previous formyl-MFR-dependent formyl/formate dehydrogenase system, which is highest expressed at the transcriptional and protein levels [18], the genome of *M. oxyfera* has the inventory of two alternative and much lower expressed systems (Figure 16a, b). Both harbor a canonical formate dehydrogenase catalytic subunit (FdhA). The first alternative (DAMO_1134-1138) seems to represent a hybrid between fMFR-DH, common formate dehydrogenase and NADH-dehydrogenase (complex I, Nuo) elements. The DAMO_1134-1138 genes form part of a larger gene cluster (DAMO_1128-1147) (Figure 16a). The cluster encodes more components required for formyl/formate/dehydrogenase functionality, such as molybdate and tungstate ABC-type transporters, a porin that might facilitate uptake of these metals, and selenocysteine and molybdopterin (MoaC) biosynthetic genes. A two-component regulatory system and ModE-type transcriptional regulator in front of the gene cluster could be involved in expression control.

Regarding the DAMO_1134-1138 formyl/formate dehydrogenase, DAMO_1134 is a FwD paralog (53 % sequence identity to DAMO_0456). DAMO_1135 and DAMO_1136 have been annotated as two genes, but the DAMO_1135 stop codon most likely represents a selenocysteine codon. Together the translated DAMO_1135-36 sequences fully cover DAMO_0457 FhcB and the FwdB subunits of the *M. kandleri* cysteine- (MK0259) and selenocysteine (MK1527) Fwds. Most notably, the presumed end of DAMO_1135 matches the position (amino acid 120) of selenocysteine in MK1527. These properties suggest a role of DAMO_1134-36 as a selenocysteine-containing fMFR-DH. In DAMO_1138, all features are conserved that have been identified in the crystal structure of *E. coli* formate dehydrogenase H (FDH-H) [132] with the binding of the molybdo-*bis*PGD prosthetic group and the preceding 4Fe4S cluster. Sequence conservation of DAMO_1138 with respect to tungsten-containing FDH from *Desulfovibrio gigas*, another enzyme of which the atomic structure has been resolved [133], is much lower (22 % identity) than with *E. coli* FDH-H (36 %). This is indicative that DAMO_1138 binds Mo at its catalytic metal. However, whereas FDH-H is a selenocysteine protein, in DAMO_1138 a cysteine is present at the equivalent position. Still, there is one more major difference. DAMO_1138 has an N-terminal extension that shows significant sequence identity with the NuoG subunit of bacterial complex I. The identity includes the presence of the set of cysteines that coordinate two 2Fe2S and two 4Fe4S clusters in NuoG [134] (Figure 16c). Otherwise, the extension is not unique for *M. oxyfera* and it is also seen in formate dehydrogenases from sulfate reducers and homoacetogens. DAMO_1137 is homologous to the beta subunit of formate dehydrogenase (FdhB). Similarly to NuoF in complex I [134], FdhB is the $NAD(P)^+$- and flavin mononucleotide (FMN)-binding subunit of FDH. Taken together, the analyses suggest that DAMO_1134-1138 is a bifunctional enzyme, capable of formylmethanofuran and of formate oxidation (eqs 19 and 20) using $NAD(P)^+$ as the electron acceptor.

The third formate dehydrogenase is the simplest one consisting of two subunits only (DAMO_0853-0854) (Figure 16). The DAMO_0853 sequence is 39.5 % identical to the DAMO_1138 FdhA subunit. This identity includes a NuoG-like N-terminal part. Similarly, in its C-terminal part DAMO_0854 displays 34 % sequence identity to DAMO_1137 FdhB. Remarkably, DAMO_0854 (710 amino

acids) is much longer than DAMO_1137 (472 amino acids). The difference concerns the presence in DAMO_0854 of the N-terminal extension that is related to the NuoE subunit [134] of the bacterial (NuoA-N) complex I. Again, the data are in agreement with a function of DAMO_0853-0854 as a $NAD(P)^+$-dependent FDH.

All this brings us to the role of formate in the metabolism of *M. oxyfera*, which could be a complex one like in methylotrophs [135]. It is known that cells of *M. oxyfera* instantaneously use exogenous formate as the electron donor for nitrite reduction and methane activation [18]. Thus, *M. oxyfera* is capable of formate uptake. Within the cells, formate can be the product of formyl-H_4F lyase (PurU) activity. Next, formate could be made by methanol dehydrogenase. MDHs not only catalyze the oxidation of methanol to formaldehyde, but also its subsequent oxidation to formate, and formaldehyde-oxidizing activity is particularly high in REE-containing XoxF MDHs [114]. Thirdly, formate might be produced by the above FwdDFhcBADC system (DAMO_0456-0460) similar to the *M. extorquens* Fhc complex (eq. 22). Extrusion of excess formate or import from the environment might serve the balancing of electron fluxes in oxidative and reductive metabolic processes. Obviously, formate movements would require an appropriate transporter, which is available in the genome as a FocA/NirC-type formate/nitrite transporter (DAMO_2284).

5 General Conclusions

For a long time, it was believed that the anaerobic oxidation of ammonium and of methane would be impossible. The reason for this was that enzymes, that were capable to break up the N-H bond of ammonium and the C-H bond of methane, depended on oxygen. From this chapter, it may have become clear that anaerobic ammonium and methane oxidizers do exist and that their existence went with the development of new enzyme systems that might involve subtle and elegant variations of metal-based catalyses that we already know from other, even completely different enzymic reactions. In anammox bacteria, ammonium is activated into hydrazine using the oxidative power of NO (see Section 3.2). In the N-DAMO process by *M. oxyfera*, a modification of a common NOR might have turned this enzyme into a machinery with another functionality, a nitric oxide dismutase generating N_2 and O_2 (see Section 4.1.3), the latter compound enabling *M. oxyfera* to utilize the same pathway for methane oxidation as aerobic methanotrophs do (see Section 4.2). While many details regarding their catalytic mechanisms still remain to be elucidated, the novel hydrazine synthase and NO dismutase are extremely slow enzymes. Obviously, the slow rate of these key enzymes immediately affects the growth rates of the microorganisms, which is very low as well. These slow growth rates, requiring dedicated enrichment techniques, may have been another reason why anammox and N-DAMO bacteria have evaded our attention. Although slow, the presence of the novel ammonium- and methane-activating systems

provides the microorganisms with a unique niche in anaerobic ecosystems, which is a central one in case of anammox bacteria [8, 11, 12].

Genome sequencing of anammox bacteria and of *M. oxyfera*, supported by a beginning of the functional characterization of enzymes involved, has been surprising and rewarding. A first surprise was the genetic redundancy of many enzymes that are related with central catabolic pathways [21, 26]. For instance, anammox bacteria harbor a core set of no less than eight to ten different HAO-like enzymes that are tuned for hydrazine and hydroxylamine oxidation, possibly for nitrite reduction and still to be discovered other functions by subtle changes around their heme *c* catalytic sites (see Section 3.3). In *M. oxyfera* five different NOR-like proteins might catalyze NO dismutation and NO reduction, again brought about by specific amino acid substitutions near the active sites (see Sections 4.1.2, 4.1.3, and 4.1.4). Besides these, anammox bacteria and *M. oxyfera* are likely to be goldmines for divergent catalytic proteins and respiratory complexes, often representing new combinations of systems that have been well-studied in current model organisms. The putative novel *bc* complexes, new complex I-formate dehydrogenase combinations and NXR systems in anammox bacteria [21, 26], and the REE-containing MDH (see Section 4.2.2.) and formate dehydrogenases (see Section 4.2.4) in *M. oxyfera* are just a few examples. However, apart from enzymes that lend anammox bacteria and *M. oxyfera* their specific ecological position, such as hydrazine synthase and hydrazine dehydrogenase, many proteins are not unique for these microorganisms. Close homologs are readily found in protein databases and in genomes assembled by metagenomic approaches, covering a variety of poorly studied or as-yet unknown environmental species.

In the end, anammox bacteria and *M. oxyfera* may stand model for a general principle: There are no such things as "impossible" microorganisms. Each biogeochemical process that is associated with a negative Gibbs free energy change finds a microbe that can thrive on the reaction. Time, a plethora of protein templates, metal-based catalytic mechanisms, and genetic toolboxes will allow the accommodation of metabolic pathways to specific needs. Their uncovering may take time as well, especially with respect to slow-growing species that are likely more the rule than the exception in natural systems.

Abbreviations and Definitions

$\Delta G^{0\prime}$ E_0'	Gibbs free energy changes and standard midpoint redox potentials, both at pH 7, were taken or calculated from data presented in [136, 137]
AMO	ammonium monooxygenase
anammox	anaerobic ammonium oxidation
AOA	ammonium-oxidizing Archaea
AOB	ammonium-oxidizing Bacteria
ATP	adenosine 5′-triphosphate
*bis*PGD	*bis*(pyrano guanine dinucleotide)

C1	one-carbon compound
cNOR	cytochrome *c*-dependent nitric oxide reductase
Cyt *c*	cytochrome *c*
DMSO	dimethylsulfoxide
DNRA	dissimilatory nitrite/ nitrate reduction forming ammonium
FAD	flavin adenine dinucleotide
Fae	formaldehyde activating enzyme
Fhc	formyl transferase/hydrolase
FDH	formate dehydrogenase
FMD	molybdenum-containing formylmethanofuran dehydrogenase
fMFR	formylmethanofuran
fMFR-DH	formylmethanofuran dehydrogenase
Fwd	tungsten-containing formylmethanofuran dehydrogenase
H_4F	5,6,7,8-tetrahydrofolate
H_4MPT	5,6,7,8-tetrahydromethanopterin
HAO	hydroxylamine oxidoreductase
HCO	heme-copper oxidase
HDH/HZO	hydrazine dehydrogenase/oxidase
HQNO	2-heptyl hydroxyquinoline N-oxide
HZS	hydrazine synthase
MCO	multicopper oxidase
MDH	methanol dehydrogenase
methanogen	Archaeon that grows by the formation of methane
methanotroph	organism capable of (aerobic) growth on methane
methylotroph	organism capable of growth on methylated compound(s)
MFR	methanofuran
MMO	methane monooxygenase
MPT	molybdopterin
$MQ(H_2)$	(reduced) menaquinone
Mtd	methylenetetrahydromethanopterin dehydrogenase
MxaFI	heterotetrameric calcium-containing methanol dehydrogenase
NAD(P)H	nicotinamide adenine dinucleotide (phosphate) reduced
N-cycle	biogeochemical nitrogen cycle
N-DAMO	nitrite-dependent anaerobic methane oxidation
N_2OR	nitrous oxide (N_2O) reductase
Nap	periplasmic dissimilatory nitrate reductase
Nar	cytoplasmic dissimilatory nitrate reductase
Nas	assimilatory nitrate reductase
NeHAO	*Nitrosomonas europaea* hydroxylamine oxidoreductase
Nir	nitrite reductase
Nrf	ammonium-forming nitrite reductase
NOD	nitric oxide dismutase
NOR	nitric oxide reductase
NXR	nitrite:nitrate oxidoreductase

pMMO	particulate membrane-bound methane monooxygenase
PQQ	pyrroloquinoline quinone
qNOR	quinol-dependent nitric oxide reductase
quinoprotein	protein containing PQQ at its active site
REE	rare earth element
sMMO	soluble methane monooxygenase
tat	twin-arginine translocation signal
TMH	transmembrane-spanning helix
XoxF	homodimeric rare earth element-containing methanol dehydrogenase

Acknowledgments The contribution by Joachim Reimann was supported by the Netherlands Organization for Scientific Research (ALW grant number 822.02.005). The work by Mike Jetten is facilitated by two European Union Advanced Research Grants (ERC 232937, ERC 339880) and by the Dutch Government "Zwaartekrachtsubsidie" (Gravitation Grant) to the Soehngen Institute for Anaerobic Microbiology (SIAM 024 002 002).

References

1. D. J. Arp, L. Y. Stein, *Crit. Rev. Biochem. Mol. Biol.* **2003**, *38*, 471–495.
2. M. A. Culpepper, A. C. Rosenzweig, *Crit. Rev. Biochem Mol. Biol.* **2012**, *47*, 483–492.
3. T. J. Lawton, J. Ham, T. Sun, A. C. Rosenzweig, *Proteins*, **2014**, *82*, 2263–2267.
4. R. Hatzenpichler, *Appl. Environ. Microbiol.* **2012,** *78*, 7501–7510.
5. W. Martens-Habbena, P. M. Berube, H. Urakawa, J. R. de la Torre, D. A. Stahl, *Nature* **2009**, *461*, 976–979.
6. N. Vajrala, W. Martens-Habbena, L. A. Sayavedra-Soto, A. Schauer, P. J. Bottomley, D. A. Stahl, D. J. Arp, *Proc. Natl. Acad. Sci. USA* **2013**, *110*, 1006–1011.
7. M. Strous, J. J. Heijnen, J. G. Kuenen, M. S. M. Jetten, *Appl. Microbiol. Biotechnol.* **1998**, *50*, 589–596.
8. M. C. Schmid, B. Maas, A. Dapena, K. van de Pas-Schoonen, J. van de Vossenberg, B. Kartal, L. van Niftrik, I. Schmidt, I. Cirpus, J. G. Kuenen, M. Wagner, J. S. Sinninghe Damsté, M. Kuypers, N. P. Revsbech, R. Mendez, M. S. M. Jetten, M. Strous, *Appl. Environ. Microbiol.* **2005**, *71*, 1677–1784.
9. (a) A. A. van de Graaf, A. Mulder, P. de Bruijn, M. S. M. Jetten, L. A. Robertson, J. G. Kuenen, *Appl. Environ. Microbiol.* **1995**, *61*, 1246–1251. (b) A. A. van de Graaf, P. de Bruijn, L. A. Robertson, M. S. M. Jetten, J. G. Kuenen, *Microbiology* **1996**, *142*, 2187–2196.
10. M. Strous, J. A. Fuerst, E. H. Kramer, S. Logemann, G. Muyzer, K.T. van de Pas-Schoonen, R. Webb, J. G. Kuenen, M. S. M. Jetten, *Nature* **1999**, *400*, 446–449.
11. H. J. M. Op den Camp, B. Kartal, D. Guven, L. A. van Niftrik, H. C. Haaijer, W. R. van der Star, K. T. van de Pas-Schoonen, A. Cabezas, Z. Ying, M. C. Schmid, M. M. Kuypers, J. van de Vossenberg, H. R. Harhangi, C. Picioreanu, M. C. van Loosdrecht, J. G. Kuenen, M. Strous, M. S. M. Jetten, *Biochem. Soc. Trans.* **2006**, *34*, 174–178.
12. B. Kartal, L. van Niftrik, J. T. Keltjens, H. J. M. Op den Camp, M. S. M. Jetten, *Adv. Microb. Physiol.* **2012**, *60*, 211–262.
13. B. Kartal, J. G. Kuenen, M. C. van Loosdrecht, *Science* **2010**, *328*, 702–703.

14. (a) K. Knittel, A. Boetius, *Annu. Rev. Microbiol.* **2009**, *63*, 311–334. (b) R. K. Thauer, *Curr. Opin. Microbiol.* **2011**, *14*, 292–299. (c) J. Milucka, T. G. Ferdelman, L. Polerecky, D. Franzke, G. Wegener, M. Schmid, I. Lieberwirth, M. Wagner, F. Widdel, M. M. Kuypers, *Nature* **2012**, *491*, 541–546. (d) T. Holler, G. Wegener, H. Niemann, C. Deusner, T. G. Ferdelman, A. Boetius, B. Brunner, F. Widdel, *Proc. Natl. Acad. Sci. USA* **2011**, *108*, E1484–1490.
15. M. F. Haroon, S. Hu, Y. Shi, M. Imelfort, J. Keller, P. Hugenholtz, Z. Yuan, G. W. Tyson, *Nature* **2013**, *500*, 567–570.
16. A. A. Raghoebarsing, A. Pol, K. T. van de Pas-Schoonen, A. J. Smolders, K. F. Ettwig, W. I. Rijpstra, S. Schouten, J. S. Damsté, H. J. M. Op den Camp, M. S. M. Jetten, M. Strous, *Nature* **2006**, *440*, 918–921.
17. K. F. Ettwig, S. Shima, K. T. van de Pas-Schoonen, J. Kahnt, M. H. Medema, H. J. M. Op den Camp, M. S. M. Jetten, M. Strous, *Environ. Microbiol.* **2008**, *10*, 3164–3173.
18. K. F. Ettwig, M. K. Butler, D. Le Paslier, E. Pelletier, S. Mangenot, M. M. Kuypers, F. Schreiber, B. E. Dutilh, J. Zedelius, D. de Beer, J. Gloerich, H. J. Wessels, T. van Alen, F. Luesken, M. L. Wu, K. T. van de Pas-Schoonen, H. J. M. Op den Camp, E. M. Janssen-Megens, K. J. Francoijs, H. Stunnenberg, J. Weissenbach, M. S. M. Jetten, M. Strous, *Nature* **2010**, *464*, 543–548.
19. (a) L. Chistoserdova, M. G. Kalyuzhnaya, M. E. Lidstrom, *Annu. Rev. Microbiol.* **2009**, *63*, 477–499. (b) L. Chistoserdova, *Environ. Microbiol.* **2011**, *13*, 2603–2622.
20. (a) A. A. van de Graaf, P. de Bruijn, L. A. Robertson, M. S. M. Jetten, J. G. Kuenen, *Microbiology* **1997,** *143*, 2415–21. (b) J. Schalk, H. Oustad, J. G. Kuenen, M. S. M Jetten, *FEMS Microbiol. Lett.* **1998**, *158*, 61–67.
21. M. Strous, E. Pelletier, S. Mangenot, T. Rattei, A. Lehner, M. W. Taylor, M. Horn, H. Daims, D. Bartol-Mavel, P. Wincker, V. Barbe, N. Fonknechten, D. Vallenet, B. Segurens, C. Schenowitz-Truong, C. Médigue, A. Collingro, B. Snel, B. E. Dutilh, H. J. M. Op den Camp, C. van der Drift, I. Cirpus, K. T. van de Pas-Schoonen, H. R. Harhangi, L. van Niftrik, M. Schmid, J. T. Keltjens, J. van de Vossenberg, B. Kartal, H. Meier, D. Frishman, M. A. Huynen, H. W. Mewes, J. Weissenbach, M. S. M. Jetten, M. Wagner, D. Le Paslier, *Nature* **2006,** *440*, 790–794.
22. B. Kartal, W. J. Maalcke, N. M. de Almeida, I. Cirpus, J. Gloerich, W. Geerts, H. J. M. Op den Camp, H. R. Harhangi, E. M. Janssen-Megens, K. J. Francoijs, H. G. Stunnenberg, J. T. Keltjens, M. S. M. Jetten, M. Strous, *Nature* **2011**, 479,127–130.
23. (a) M. R. Lindsay, R. I. Webb, M. Strous, M. S. M. Jetten, M. K. Butler, R. J. Forde, J. A. Fuerst, *Arch. Microbiol.* **2001**, *175*, 413–429. (b) L. A. van Niftrik, J. A. Fuerst, J. S. Sinninghe Damsté, J. G. Kuenen, M. S. M. Jetten, M. Strous, *FEMS Microbiol. Lett.* **2004**, *233*, 7–13. (c) L. van Niftrik, W. J. Geerts, E. G. van Donselaar, B. M. Humbel, A. Yakushevska, A. J. Verkleij, M. S. M. Jetten, M. Strous, *J. Struct. Biol.* **2008**, *161*, 401–410. (d) L. van Niftrik, W. J. Geerts, E. G. van Donselaar, B. M. Humbel, R. I. Webb, J. A. Fuerst, A. J. Verkleij, M. S. M. Jetten, M. Strous, *J. Bacteriol.* **2008**, *190*, 708–717.
24. (a) L. van Niftrik, M. van Helden, S. Kirchen, E. G. van Donselaar, H. R. Harhangi, R. I. Webb, J. A. Fuerst, H. J. M. Op den Camp, M. S. M. Jetten, M. Strous, *Mol. Microbiol.* **2010**, *77*, 701–715. (b) R. Karlsson, A. Karlsson, O. Bäckman, B. R. Johansson, S. Hulth, *FEMS Microbiol. Lett.* **2009**, *297*, 87–94. (c) R. Karlsson, A. Karlsson, O. Bäckman, B. R. Johansson, S. Hulth, *FEMS Microbiol. Lett.* **2014**, *354*, 10–18.
25. L. van Niftrik, M. S. M. Jetten, *Microbiol. Mol. Biol. Rev.* **2012**, *76*, 585–596.
26. B. Kartal, N. M. de Almeida, W. J. Maalcke, H. J. M. Op den Camp, M. S. M. Jetten, J. T. Keltjens, *FEMS Microbiol. Rev.* **2013**, *37*, 428–461.
27. N. M. de Almeida, W. J. Maalcke, J. T. Keltjens, M. S. M. Jetten, B. Kartal B, *Biochem. Soc. Trans.* **2011**, *39*, 303–308.
28. (a) B. Kartal, J. Rattray, L. A. van Niftrik, J.van de Vossenberg, M. C. Schmid, R. I. Webb, S. Schouten, J. A. Fuerst, J.S. Sinninghe Damsté, M. S. M. Jetten, M. Strous, *Syst. Appl. Microbiol.* **2007**, *30*, 39–49. (b) B. Kartal, M. M. M. Kuypers, G. Lavik, J. Schalk, H. J. M. Op

den Camp, M. S. M. Jetten, M. Strous, *Environ. Microbiol.* **2007**, *9*, 635–642. (c) B. Kartal, L. van Niftrik, J. Rattray, J. L.van de Vossenberg, M. C. Schmid, J. Sinninghe Damsté, M. S. M. Jetten, M. Strous, *FEMS Microbiol. Ecol.* **2008**, *63*, 46–55.
29. M. L. Wu, S. de Vries S, T. A. van Alen, M. K. Butler, H. J. M. Op den Camp, J. T. Keltjens, M. S. M. Jetten, M. Strous, *Microbiology* **2011**, *157*, 890–898.
30. (a) S. J. Ferguson, V. Fülöp, *Subcell. Biochem.* **2000**, *35*, 519–540. (b) O. Einsle, P. M. H. Kroneck, *Biol. Chem.* **2004,** *385*, 875–883. (c) P. Tavares, A. S. Pereira, J. J. Moura, I. Moura, *J. Inorg. Biochem.* **2006**, *100*, 2087–2100. (d) I. S. MacPherson, M. E. Murphy, *Cell. Mol. Life Sci.* **2007**, *64*, 2887–2899. (e) S. Rinaldo A. Arcovito, G. Giardina, N. Castiglione, M. Brunori, F. Cutruzzolà, *Biochem. Soc. Trans.* **2008**, *36*, 1155–1159. (f) A. C. Merkle, N. Lehnert, *Dalton Trans.* **2012**, *41*, 3355–3368.
31. (a) P. A. Williams, V. Fülöp, E. F. Garman, N. F. Saunders, S. J. Ferguson, J. Hajdu, *Nature* **1997**, 389, 406–412. (b) D. Nurizzo, M. C. Silvestrini, M. Mathieu, F. Cutruzzolà, D. Bourgeois, V. Fülöp V, J. Hajdu, M. Brunori, M. Tegoni, C. Cambillau, *Structure* **1997**, *5*, 1157–1171. (c) D. Nurizzo, F. Cutruzzolà, M. Arese, D. Bourgeois, M. Brunori, C. Cambillau, M. Tegoni, *Biochemistry* **1998**, *37*, 13987–13996.
32. (a) S. Kawasaki, H. Arai, T. Kodama, Y. Igarashi, *J. Bacteriol.* **1997**, *179*, 235–242. (b) S. Bali, A. D. Lawrence, S. A. Lobo, L. M. Saraiva, B. T. Golding, D. J. Palmer, M. J. Howard, S. J. Ferguson, M. J. Warren, *Proc. Natl. Acad. Sci. USA* **2011**, *108*, 18260–18265.
33. J. van de Vossenberg, D. Woebken, M. J. Maalcke, H. J. Wessels, B. E. Dutilh, B. Kartal, E. M. Janssen-Megens, G. Roeselers, J. Yan, D. Speth, J. Gloerich, W. Geerts, E. van der Biezen, W. Pluk, K. J. Francoijs, L. Russ, P. Lam, S. A. Malfatti, S. G. Tringe, S. C. Haaijer, H. J. M. Op den Camp, H. G. Stunnenberg, R. Amann, M. M. Kuypers, M. S. M. Jetten, *Environ Microbiol.* **2013**, *15*, 1275–1289.
34. D. Hira, H. Toh, C. T. Migita, H. Okubo, T. Nishiyama, M. Hattori, K. Furukawa, T. Fujii, *FEBS Lett.* **2012**, *586*, 1658–1663.
35. Z. Hu D. R. Speth, K. J. Francoijs, Z. X. Quan, M. S. M. Jetten, *Front. Microbiol.* **2012**, *3*, 366.
36. F. Gori, S. G. Tringe, B. Kartal, E. Marchiori M. S. M. Jetten, *Biochem. Soc. Trans.* **2011**, *39*, 1799–1804.
37. (a) G. W. Pettigrew, A. Echalier, S. R. Pauleta, *J. Inorg. Biochem.* **2006**, *100*, 551–567. (b) J. M. Atack, D. J. Kelly, *Adv. Microb. Physiol.* **2007**, *52*, 73–106.
38. (a) C. M. Wilmot, V. L. Davidson, *Curr. Opin. Chem. Biol.* **2009**, *13*, 469–474. (b) C. M. Wilmot, E. T. Yukl, *Dalton. Trans.* **2013**, **42**, 3127–3135. (c) S. Shin S, V. L. Davidson, *Arch. Biochem. Biophys.* **2014**, *544C*, 112–118.
39. (a) S. L. Edwards, T. L. Poulos, *J. Biol. Chem.* **1990**, *265*, 2588–2595. (b) E. T. Yukl, B. R. Goblirsch, V. L. Davidson, C. M. Wilmot, *Biochemistry* **2011**, *50*, 2931–2938.
40. M. Jormakka, S. Törnroth, B. Byrne, S. Iwata, *Science* **2002**, *295*, 1863–1868.
41. (a) A. B. Hooper, A. Nason, *J. Biol. Chem.* **1965**, *240*, 4044–4057. (b) K. R. Terry, A. B. Hooper, *Biochemistry* **1981**, *20*, 7026–7032.
42. A. B. Hooper, T. Vannelli, D. J. Bergmann, D. M. Arciero, *Antonie Van Leeuwenhoek* **1997**, *71*, 59–67.
43. (a) N. Igarashi, H. Moriyama, T. Fujiwara, Y. Fukumori, N. Tanaka, *Nat. Struct. Biol.* **1997**, *4*, 276–284. (b) P. E. Cedervall, A. B. Hooper, C. M. Wilmot, *Acta Crystallogr. Sect F Struct. Biol. Cryst. Commun.* **2009**, *65*, 1296–1298. (c) P. Cedervall, A. B. Hooper, C. M. Wilmot, *Biochemistry* **2013**, *52*, 6211–6218.
44. W. J. Maalcke, A. Dietl, S. J. Marritt, J. N. Butt, M. S. M. Jetten, J. T. Keltjens, T. R. Barends, B. Kartal, *J. Biol. Chem.* **2014**, *289*, 1228–1242.
45. (a) M. G. Klotz, M. C. Schmid, M. Strous, H. J. M. op den Camp, M. S. M. Jetten, A. B. Hooper, *Environ. Microbiol.* **2008**, *10*, 3150–3163. (b) J. Simon, M. G. Klotz, *Biochim. Biophys. Acta* **2013**, *1827*, 114–135.
46. M. Shimamura, T. Nishiyama, K. Shinya, Y. Kawahara, K. Furukawa, T. Fujii, *J. Biosci. Bioeng.* **2008**, *105*, 243–248.

47. J. Schalk, S. de Vries, J. G. Kuenen, M. S. M. Jetten, *Biochemistry* **2000**, *39*, 5405–5412.
48. W. L. DeLano, *The PyMOL Molecular Graphics System*, DeLano Scientific, San Carlos, CA, USA, 2002, http://www.pymol.org.
49. M. L. Fernández, D. A. Estrin, S. E. Bari, *J. Inorg. Biochem.* **2008**, *102*, 1523–1530.
50. M. Shimamura, T. Nishiyama, H. Shigetomo, T. Toyomoto, Y. Kawahara, K. Furukawa, T. Fujii, *Appl. Environ. Microbiol.* **2007**, *73*, 1065–1072.
51. W. J. Maalcke, *Multiheme Protein Complexes of Anaerobic Ammonium-Oxidizing Bacteria*, PhD Thesis, Radboud University of Nijmegen (The Netherlands), 2012.
52. (a) J. Kostera, J. McGarry, A. A. Pacheco, *Biochemistry* **2010**, *49*, 8546–8553. (b) A. A. Pacheco, J. McGarry, J. Kostera, A. Corona, *Methods Enzymol.* **2011**, *486*, 447–463.
53. (a) H. B. Gray, B. G. Malmström, R. J. P. Williams, *J. Biol. Inorg. Chem.* **2000**, *5*, 551–559. (b) H. B. Gray, J. R. Winkler, *Biochim. Biophys. Acta* **2010**, *1797*, 1563–1572. (c) M. Choi, V. L. Davidson, *Metallomics* **2011**, *3*, 140–151.
54. (a) I. V. Pearson, M. D. Page, R. J. van Spanning, S. J. Ferguson, *J. Bacteriol.* **2003**, *185*, 6308–6315. (b) K. A. Sam, S. A. Fairhurst, R. N. Thorneley, J. W. Allen, S. J. Ferguson, *J. Biol. Chem.* **2008**, *283*, 12555–12563.
55. F. ten Brink, B. Schoepp-Cothenet, R. van Lis, W. Nitschke, F. Baymann, *Biochim. Biophys. Acta* **2013**, *1827*, 1392–1406.
56. D. V. Dibrova, D. A. Cherepanov, M. Y. Galperin, V. P. Skulachev, A. Y. Mulkidjanian, *Biochim. Biophys. Acta* **2013**, *1827*, 1407–1427.
57. (a) X. Gao, X. Wen, L. Esser, B. Quinn, L. Yu, C. A. Yu, D. Xia, *Biochemistry* **2003**, *42*, 9067–9080. (b) X. Gao, X. Wen, C. Yu, L. Esser, S. Tsao, B. Quinn, L. Zhang, L. Yu, D. Xia, *Biochemistry* **2002**, *41*, 11692–11702. (c) H. Palsdottir, C. G. Lojero, B. L. Trumpower, C. Hunte, *J. Biol. Chem.* **2003**, *278*, 31303–31311. (d) L. Esser, B. Quinn, Y. F. Li, M. Zhang, M. Elberry, L. Yu, C. A. Yu, D. Xia, *J. Mol. Biol.* **2004**, *341*, 281–302. (e) L. Esser, M. Elberry, F. Zhou, C. A. Yu, L. Yu, D. Xia, *J. Biol. Chem.* **2008**, *283*, 2846–2857. (f) S. R. Solmaz, C. Hunte, *J. Biol. Chem.* **2008**, *283*, 17542–17549. (g) J. Yan, G. Kurisu, W. A. Cramer, *Proc. Natl. Acad. Sci. USA* **2006**, *103*, 69–74. (h) E. Yamashita, H. Zhang, W. A. Cramer, *J. Mol. Biol.* **2007**, *370*, 39–52.
58. (a) H. Claus, *Arch. Microbiol.* **2003**, *179*, 145–150. (b) P. Giardina, V. Faraco, C. Pezzella, A. Piscitelli, S. Vanhulle, G. Sannia, *Cell. Mol. Life Sci.* **2010**, *67,* 369–385. (c) P. Di Gennaro, A. Bargna, G. Sello, *Appl. Microbiol. Biotechnol.* **2011**, *90***,** 1817–1827.
59. (a) M. C. Machczynski, E. Vijgenboom, B. Samyn, G. W. Canters, *Protein Sci* **2004**, *13***,** 2388–2397. (b) T. Skálová, J. Dohnálek, L. H. Østergaard, P. R. Østergaard, P. Kolenko, J. Dusková, A. Stepánková, J. Hasek, *J. Mol. Biol.* **2009**, *385***,** 1165–1178.
60. M. Sutter, D. Boehringer, S. Gutmann, S. Günther, D. Prangishvili, M. J. Loessner, K. O. Stetter, E. Weber-Ban, N. Ban, *Nat. Struct. Mol. Biol.* **2008**, *15***,** 939–947.
61. R. A. Rothery, G. J. Workun, J. H. Weiner, *Biochim. Biophys. Acta* **2008**, *1778***,** 1897–1929.
62. M. Jormakka, D. Richardson, B. Byrne, S. Iwata, *Structure* **2004**, *12*, 95–104.
63. S. Lücker, M. Wagner, F. Maixner, E. Pelletier, H. Koch, B. Vacherie, T. Rattei,J. S. Damsté, E. Spieck, D. Le Paslier, H. Daims, *Proc. Natl. Acad. Sci. USA* **2010**, 107, 13479–13484.
64. S. Lücker, B. Nowka, T. Rattei, E. Spieck, H. Daims, *Front. Microbiol.* **2013**, *4*, 27.
65. M. G. Bertero, R. A. Rothery, M. Palak, C. Hou, D. Lim, F. Blasco, J. H. Weiner, N. C. Strynadka, *Nature Struct. Mol. Biol.* **2003**, *10***,** 681–687.
66. C. A. McDevitt, G. R. Hanson, C. J. Noble, M. R. Cheesman, A. G. McEwan, *Biochemistry* **2002**, *41*, 15234–15244.
67. (a) I. Schröder, S. Rech, T. Krafft, J. M. Macy, *J. Biol. Chem.* **1997**, *272*, 23765–23768. (b) E. C. Lowe, S. Bydder, R. S. Hartshorne, H. L. Tape, E. J. Dridge, C. M. Debieux, K. Paszkiewicz, I. Singleton, R. J. Lewis, J. M. Santini, D. J. Richardson, C. S. Butler, *J. Biol. Chem.* **2010**, 285, 18433–18442.
68. H. D. Thorell, K. Stenklo, J. Karlsson, T. Nilsson, *Appl. Environ. Microbiol.* **2003**, *69*, 5585–5592.
69. D. P. Kloer, C. Hagel, J. Heider, G. E. Schulz, *Structure* **2006**, *14*, 1377–1388.

70. (a) P. Lanciano, A. Vergnes, S. Grimaldi, B. Guigliarelli, A. Magalon, *J. Biol. Chem.* **2007**, *282*, 17468–17474. (b) S. Zakian, D. Lafitte, A. Vergnes, C. Pimentel, C. Sebban-Kreuzer, R. Toci, J. B. Claude, F. Guerlesquin, A. Magalon, *FEBS J.* **2010**, *277*, 1886–1895.
71. (a) V. B. Borisov, R. B. Gennis, J. Hemp, M. I. Verkhovsky, *Biochim. Biophys. Acta* **2011**, *1807*, 1398–1413. (b) A. Giuffrè, V. B. Borisov, M. Arese, P. Sarti, E. Forte, *Biochim. Biophys. Acta* **2014**, *1837*, 1178–1187.
72. S. B. Mohan, M. Schmid, M. S. M. Jetten, J. Cole, *FEMS Microbiol. Ecol.* **2004**, *49*, 433–443.
73. (a) J. Simon, M. Kern, *Biochem. Soc. Trans.* **2008**, *36*, 1011–1016. (b) M. Kern, J. Simon, *Biochim. Biophys. Acta* **2009**, *1787*, 646–656.
74. (a) O. Einsle, A. Messerschmidt, P. Stach, G. P. Bourenkov, H. D. Bartunik, R. Huber, P. M. H. Kroneck, *Nature* **1999**, *400***,** 476–480. (b) O. Einsle, A. Messerschmidt, R. Huber, P. M. H. Kroneck, F. Neese, *J. Am. Chem. Soc.* **2002**, *124*, 11737–11745.
75. M. J. Sellars, S. J. Hall, D. J. Kelly, *J. Bacteriol.* **2002**, *184*, 4187–4196.
76. R. A. Sanford, J. R. Cole, J. M. Tiedje, *Appl. Environ. Microbiol.* **2002**, *68*, 893–900.
77. (a) M. S. Pittman, K. T. Elvers, L. Lee, M. A. Jones, R. K. Poole, S. F. Park, D. J. Kelly, *Mol. Microbiol.* **2007**, *63*, 575–590. (b) M. Kern, F. Eisel, J. Scheithauer, R. G. Kranz, J. Simon, *Mol. Microbiol.* **2010**, *75*, 122–137.
78. A. Welsh, J. Chee-Sanford, L. Connor, F. Löffler, R. Sanford, *Appl. Environ. Microbiol.* **2014**, *80*, 2110–2119.
79. (a) K. M. Polyakov, K. M. Boyko, T. V. Tikhonova, A. Slutsky, A. N. Antipov, R. A. Zvyagilskaya, A. N. Popov, G. P. Bourenkov, V. S. Lamzin, V. O. Popov, *J. Mol. Biol.* **2009**, *389*, 846–862. (b) A. A. Trofimov, K. M. Polyakov, K. M. Boyko, T. V. Tikhonova, T. N. Safonova, A. V. Tikhonov, A. N. Popov, V. O. Popov, *Acta Crystallogr. D Biol. Crystallogr.* **2010**, *66*, 1043–1047. (c) T. Tikhonova, A. Tikhonov, A. Trofimov, K. Polyakov, K. Boyko, E. Cherkashin, T. Rakitina, D. Sorokin, V. Popov, *FEBS J.* **2012**, *279*, 4052–4061. (d) T. V. Tikhonova, A. A. Trofimov, V. O. Popov, *Biochemistry (Moscow)* **2012**, *77*, 1129–1138.
80. (a) C. G. Mowat, E. Rothery, C. S. Miles, L. McIver, M. K. Doherty, K. Drewette, P. Taylor, M. D. Walkinshaw, S. K. Chapman, G. A. Reid, *Nature Struct. Mol. Biol.* **2004**, *11*, 1023–1024. (b) S. J. Atkinson, C. G. Mowat, G. A. Reid, S. K. Chapman*, FEBS Lett.* **2007**, *581*, 3805–3808.
81. (a) J. J. Moura, C. D. Brondino, J. Trincão, M. J. Romão, *J. Biol. Inorg. Chem.* **2004**, *9*, 791–799. (b) G. Fritz, O. Einsle, M. Rudolf, A. Schiffer, P. M. H. Kroneck, *J. Mol. Microbiol. Biotechnol.* **2005**, *10*, 223–233. (b) P. J. González, C. Correia, I. Moura, C. D. Brondino, J. J. Moura, *J. Inorg. Biochem.* **2006**, *100*, 1015–1023. (c) J. Simon, R. J. van Spanning, D. J. Richardson, *Biochim. Biophys. Acta* **2008**, *1777*, 1480–1490. (d) B. Kraft, M. Strous, H. E. Tegetmeyer, *J Biotechnol.* **2011**, *155***,** 104–117. (e) C. Sparacino-Watkins, J. F. Stolz, P. Basu, *Chem. Soc. Rev.* **2014**, *43*, 676–706.
82. (a) J. M. Dias, M. E. Than, A. Humm, R. Huber, G. P. Bourenkov, H. D. Bartunik, S. Bursakov, J. Calvete, J. Caldeira, C. Carneiro, J. J. Moura, I. Moura, M. Romão, *Structure* **1999**, *7*, 65–79. (b) P. Arnoux, M. Sabaty, J. Alric, B. Frangioni, B. Guigliarelli, J. M. Adriano, D. Pignol, *Nat. Struct. Biol.* **2003**, *10*, 928–934. (c) B. J. Jepson, S. Mohan, T. A. Clarke, A. J. Gates, J. A. Cole, C. S. Butler, J. N. Butt, A. M. Hemmings, D. J. Richardson, *J. Biol. Chem.* **2007**, *282*, 6425–6437. (d) S. Najmudin, P. J. González, J. Trincão, C. Coelho, A. Mukhopadhyay, N. M. Cerqueira, C. C. Romão, I. Moura, J. J. Moura, C. D. Brondino, M. J. Romão, *J. Biol. Inorg. Chem.* **2008**, *13*, 737–753. (e) C. Coelho, P. J. González, J. G. Moura, I. Moura, J. Trincão, M. J. Romão, *J. Mol. Biol.* **2011***, 408*, 932–948.
83. B. Ize, S. J. Coulthurst, K. Hatzixanthis, I. Caldelari, G. Buchanan, E. C. Barclay, D. J. Richardson, T. Palmer, F. Sargent, *Microbiology* **2009**, *155*, 3992–4004.
84. (a) T. H. Brondijk, D. Fiegen, D. J. Richardson, J. A. Cole, *Mol. Microbiol.* **2002**, *44*, 245–255. (b) T. H. Brondijk, A. Nilavongse, N. Filenko, D. J. Richardson, J. A. Cole, *Biochem. J.* **2004**, *379*, 47–55. (c) A. Nilavongse, T. H. Brondijk, T. W. Overton, D. J.

Richardson, E. R. Leach, J. A. Cole, *Microbiology* **2006**, *152*, 3227–3237. (d) M. Kern, J. Simon, *Microbiology* **2009**, *155*, 2784–2794. (e) M. Kern, J. Simon, *Mol. Microbiol.* **2008**, *69*, 1137–1152.
85. (a) T. Sjögren, M. Svensson-Ek, J. Hajdu, P. Brzezinski, *Biochemistry* **2000**, *39*, 10967–10974. (b) A. Jafferji, J. W. Allen, S. J. Ferguson, V. Fulop, *J. Biol. Chem.* **2000**, *275*, 25089–25094.
86. M. L. Wu, T. A. van Alen, E. G. van Donselaar, M. Strous, M. S. M. Jetten, L. van Niftrik, *FEMS Microbiol. Lett.* **2012**, *334*, 49–56.
87. R. J. Schulze, J. Komar, M. Botte, W. J. Allen, S. Whitehouse, V. A. Gold, A. Lycklama, J. A. Nijeholt, K. Huard, I. Berger, C. Schaffitzel, I. Collinson, *Proc. Natl. Acad. Sci. USA* **2014**, *111*, 4844–4849.
88. V. M. Luque-Almagro, A. J. Gates, C. Moreno-Vivián, S. J. Ferguson, D. J. Richardson, M. D. Roldán, *Biochem. Soc. Trans.* **2011**, *39*, 1838–1843.
89. P. J. Simpson, D. J. Richardson, R. Codd, *Microbiology* **2010**, *156*, 302–312.
90. (a) L. Philippot, *Trends Microbiol.* **2005,** *13*, 191–192. (b) R. Cramm, R. A. Siddiqui, B. Friedrich, *J. Bacteriol.* **1997**, *179*, 6769–6777.
91. (a) W. G. Zumft, *J. Inorg. Biochem.* **2005**, *99*, 194–215. (b) J. Hendriks, A. Oubrie, J. Castresana, A. Urbani, S. Gemeinhardt, M. Saraste, *Biochim. Biophys. Acta* **2000**, *1459*, 266–273.
92. (a) Y. Matsumoto, T. Tosha, A. V. Pisliakov, T. Hino, H. Sugimoto, S. Nagano, Y. Sugita, Y. Shiro, *Nature Struct. Mol. Biol.* **2012**, *19*, 238–245. (b) T. Hino, Y. Matsumoto, S. Nagano, H. Sugimoto, Y. Fukumori, T. Murata, S. Iwata, *Science* **2010**, *330*, 1666–1670.
93. Suharti, M. J. F. Strampraad, I. Schröder, S. de Vries, *Biochemistry* **2001**, *40*, 2632–2639.
94. K. Heylen, J.T. Keltjens, *Front. Microbiol.* **2012**, *3*, 371.
95. J. Hemp, R. B. Gennis, *Results Probl. Cell Differ.* **2008**, *45*, 1–31.
96. (a) M. Saraste, J. Castresana, *FEBS Lett.* **1994**, *341*, 1–4. (b) J. van der Oost, A. P. N. de Boer, I.-W. L. Gier, W. G. Zumft, A. H. Stouthamer, R. J. M. van Spanning, *FEMS Microbial. Lett.* **1994**, *121*, l–10.
97. (a) T. Fujiwara, Y. Fukumori, *J. Bacteriol*, **1996**. *178*, 1866–1871. (b) U. Flock, N. J. Watmough, P. Ädelroth, *Biochemistry* **2005**, *44*, 10711–10719. (c) G. Butland, S. Spiro, N. J. Watmough, D. J. Richardson, *J. Bacteriol.* **2001**, *183*, 189–199. (d) N. Sakurai, T. Sakurai, *Biochemistry* **1997**, *36*, 13809–13815. (e) A. Giuffrè, G. Stubauer, P. Sarti, M. Brunori, W. G. Zumft, G. Buse, T. Soulimane, *Proc. Natl. Acad. Sci. USA* **1999**, *96*, 14718–14723. (f) E. Forte, A. Urbani, M. Saraste, P. Sarti, M. Brunori, A. Giuffrè, *Eur. J. Biochem.* **2001***, 268*, 6486–6491.
98. (a) D. A. Proshlyakov, M. A. Pressler, C. DeMaso, J. F. Leykam, D. L. deWitt, G. T. Babcock, *Science* **2000**, *290*, 1588–1591. (b) R. B. Gennis, *Biochim. Biophys. Acta* **1998**, *1365*, 241–248. (c) G. T. Babcock, *Proc. Natl. Acad. Sci. USA* **1999**, *96*, 12971–12973 (d) M. R. A. Blomberg, P. E. M. Siegbahn, M. Wikström, *Inorg. Chem.* **2003**, *42*, 5231–5243. (e) M. Iwaki, A. Puustinen, M. Wikström, P. R. Rich, *Biochemistry* **2003**, *42*, 8809–8817.
99. K. F. Ettwig, D. R. Speth, J. Reimann, M. L. Wu, M. S. M. Jetten, J. T. Keltjens, *Front. Microbiol.* **2012**, *3*, 273.
100. (a) F. H. Thorndycroft, G. Butland, D. J. Richardson, N. J. Watmough, *Biochem. J.* **2007**, *401*, 111–119. (b) U. Flock, P. Lachmann, J. Reimann, N. J. Watmough, P. Ädelroth, *J. Inorg. Biochem.* **2009**, *103*, 845–850.
101. (a) P. Ehrenreich, A. Behrends, J. Harder, F. Widdel, *Arch. Microbiol.* **2000**, *173*, 58–64. (b) J. Zedelius, R. Rabus, O. Grundmann, I. Werner, D. Brodkorb, F. Schreiber, P. Ehrenreich, A. Behrends, H. Wilkes, M. Kube, R. Reinhardt, F. Widdel, *Environ. Microbiol. Rep.* **2010**, *3*, 125–135.
102. L. Salomonsson, J. Reimann, T. Tosha, N. Krause, N. Gonska, Y Shiro, P. Ädelroth, *Biochim. Biophys. Acta* **2012**, *1817*, 1914–1920.

103. (a) R. L. Lieberman, A. C. Rosenzweig, *Nature* **2005**, *434*, 177–182. (b) A. S. Hakemian, K. C. Kondapalli, J. Telser, B. M. Hoffman, T. L. Stemmler, A. C. Rosenzweig, *Biochemistry* **2008**, *47*, 6793–6801. (c) S. M. Smith, S. Rawat, J. Telser, B. M. Hoffman, T. L. Stemmler, A. C. Rosenzweig, *Biochemistry* **2011**, *50*, 10231–10340.
104. R. Balasubramanian, S. M. Smith, S. Rawat, L. A. Yatsunyk, T. L. Stemmler, A. C. Rosenzweig, *Nature* **2010**, *465*, 115–119.
105. (a) H. J. Hektor, H. Kloosterman, L. Dijkhuizen, *J. Mol. Catal. B* **2000**, *8*, 103–109. (b) H. J. Hektor, H. Kloosterman, L. Dijkhuizen, *J. Biol. Chem.* **2002**, *277*, 46966–46973.
106. (a) C. Anthony, M. Ghosh, *Prog. Biophys. Mol. Biol.* **1998**, *69*, 1–21. (b) C. Anthony, P. Williams, *Biochim. Biophys. Acta* **2003**, *1647*, 18–23. (c) C. Anthony, *Arch. Biochem. Biophys*. **2004**, *428*, 2–9.
107. (a) L. Masgrau, J. Basran, P. Hothi, M. J. Sutcliffe, N. S. Scrutton, *Arch. Biochem. Biophys.* **2004**, *428*, 41–51. (b) S. Y. Reddy, T. C. Bruice, *J. Am. Chem. Soc***. 2003**, *125*, 8141–8150. (c) V. L. Davidson, *Arch. Biochem. Biophys*. **2004**, *428*, 32–40. (d) S. Y. Reddy, T. C. Bruice, *Protein Sci*. **2004**, *13*, 1965–1978. (e) X. Zhang, S. Y. Reddy, T. C. Bruice, *Proc. Natl. Acad. Sci. USA* **2007**, *104*, 745–749.
108. (a) A. Oubrie, B. W. Dijkstra, *Protein Sci*. **2000**, *9*, 1265–1273. (b) A. Oubrie, H. J. Rozeboom, K. H. Kalk, E. G. Huizinga, B. W. Dijkstra, *J. Biol. Chem.* **2002**, *277*, 3727–3732.
109. (a) Z. X. Xia, W. W. Dai, J. P. Xiong, Z. P. Hao, V. L. Davidson, S. White, F. S. Mathews, *J. Biol. Chem.* **1992**, *267*, 22289–22297. (b) Z. Xia, W. Dai, Y. Zhang, S. A. White, G. D. Boyd, F. S. Mathews, *J. Mol. Biol*. **1996**, *259*, 480–501. (c) Z. X. Xia Y. N. He, W. W. Dai, S. A. White, G. D. Boyd, F. S. Mathews, *Biochemistry* **1999**, *38*, 1214–1220. (d) Z. X. Xia, W. W. Dai, Y. N. He, S. A. White, F. S. Mathews, V. L. Davidson, *J. Biol. Inorg. Chem.* **2003**, *8*, 843–854. (e) M. Ghosh, C. Anthony, K. Harlos, M. G. Goodwin, C. Blake, *Structure* **1995**, *3*, 177–187. (f) M. Ghosh, A. Avezoux, C. Anthony, K. Harlos, C. C. Blake, *Experientia* **1994**, *71*, 251–260. (g) P. A. Williams, L. Coates, F. Mohammed, R. Gill, P. T. Erskine, A. Coker, S. P. Wood, C. Anthony, J. B. Cooper, *Acta Crystallogr. D Biol. Crystallogr*. **2005**, *61*, 75–79. (h) J. M. Choi, H. G. Kim, J. S. Kim, H. S. Youn, S. H. Eom, S. L. Yu, S. W. Kim, S. H. Lee, *Acta Crystallogr. Sect. F Struct. Biol. Cryst. Commun*. **2011**, *67*, 513–516.
110. (a) D. J. Anderson, C. J. Morris, D. N. Nunn, C. Anthony, M. E. Lidstrom, *Gene* **1990**, *90*, 173–176. (b) C. J. Morris, Y. M. Kim, K. E. Perkins, M. E. Lidstrom, *J. Bacteriol*. **1995**, *177*, 6825–6831. (c) L. Chistoserdova, S. W. Chen, A. Lapidus, M. E. Lidstrom, *J. Bacteriol*. **2003**, *185*, 2980–2987.
111. (a) N. Goosen, R. G. M. Huinen, P. Vandeputte, *J. Bacteriol*. **1992**, *174*, 1426–1427. (b) S. Puehringer, M. Metlitzky, R. Schwarzenbacher, *BMC Biochemistry* **2008**, *9*, 8. (c) N. Gliese, V. Khodaverdi, H. Görisch, *Arch. Microbiol*. **2010**, *192*, 1–14.
112. M. L. Wu, K. F. Ettwig, M. S. M. Jetten, M. Strous, J. T. Keltjens, L. van Niftrik, *Biochem. Soc. Trans*. **2011**, *39*, 243–248.
113. (a) Y. Hibi, K. Asai, H. Arafuka, M. Hamajima, T. Iwama, K. Kawai, *J. Biosci. Bioeng*. **2011**, *111*, 547–549. (b) N. A. Fitriyanto, M. Fushimi, M. Matsunaga, A. Pertiwiningrum, T. Iwama, K. Kawai, *J. Biosci. Bioeng*. **2011**, *111*, 613–617. (c) T. Nakagawa, R. Mitsui, A. Tani, K. Sasa, S. Tashiro, T. Iwama, T. Hayakawa, K. Kawai, *PloS One* **2012**, *7*, e50480.
114. A. Pol, T. R. M. Barends, A. Dietl, A. F. Khadem, J. Eygensteyn, M. S. M. Jetten, H. J. M. op den Camp, *Environ. Microbiol*. **2014**, *16*, 255–264.
115. J. T. Keltjens, A. Pol, J. Reimann, H. J. M. op den Camp, *Appl. Microbiol. Biotechnol*. **2014**, *98*, 6163–6183.
116. M. L. Wu, H. J. C. T. Wessels, A. Pol, H. J. M. Op den Camp, M. S. M. Jetten, L. Van Niftrik, J. T. Keltjens, **2014**, *submitted for publication*.
117. (a) L. Chistoserdova, J. A. Vorholt, R. K. Thauer, M. E. Lidstrom, *Science* **1998**, *281*, 99–102. (b) J. A. Vorholt, L. Chistoserdova, S. M. Stolyar, R. K. Thauer, M. E. Lidstrom, *J. Bacteriol*. **1999**, *181*, 5750–5757. (c) L. Chistoserdova, J. A. Vorholt, M. E. Lidstrom, *Genome Biol*. **2005**, *6*, 208. (d) L. Chistoserdova, M. E. Rasche, M. E. Lidstrom, *J. Bacteriol*. **2005**, *187*, 2508–2512. (e) M. G. Kalyuzhnaya, N. Korotkova, G. Crowther, C. J. Marx,

M. E. Lidstrom, *J. Bacteriol.* **2005**, *187*, 4607–4614. (f) M. G. Kalyuzhnaya, L. Chistoserdova, *Methods Enzymol.* **2005**, *397*, 443–54. (g) M. G. Kalyuzhnaya, O. Nercessian, A. Lapidus, L. Chistoserdova, *Environ. Microbiol.* **2005**, *7*, 1909–1916. (h) M. G. Kalyuzhnaya, S. Bowerman, O. Nercessian, M. E. Lidstrom, L. Chistoserdova, *Appl. Environ. Microbiol.* **2005**, *71*, 8846–8854. (i) L. Chistoserdova, A. Lapidus, C. Han, L. Goodwin, L. Saunders, T. Brettin, R. Tapia, P. Gilna, S. Lucas, P. M. Richardson, M. E. Lidstrom, *J. Bacteriol.* **2007**, *189*, 4020–4027. (j) S. Vuilleumier, L. Chistoserdova, M. C. Lee, F. Bringel, A. Lajus, Y. Zhou, B. Gourion, V. Barbe, J. Chang, S. Cruveiller, C. Dossat, W. Gillett, C. Gruffaz, E. Haugen, E. Hourcade, R. Levy, S. Mangenot, E. Muller, T. Nadalig, M. Pagni, C. Penny, R. Peyraud, D. G. Robinson, D. Roche, Z. Rouy, C. Saenampechek, G. Salvignol, D. Vallenet, Z. Wu, C. J. Marx, J. A. Vorholt, M. V. Olson, R. Kaul, J. Weissenbach, C. Médigue, M. E. Lidstrom, *PLoS One* **2009**, *4*, e5584. (k) M. G. Kalyuzhnaya, D. A. Beck, D. Suciu, A. Pozhitkov, M. E. Lidstrom, L. Chistoserdova, *ISME J.* **2010**, *4*, 388–398. (l) E. L. Hendrickson, D. A. Beck, T. Wang, M. E. Lidstrom, M. Hackett, L. Chistoserdova, *J. Bacteriol.* **2010**, *192*, 4859–4867.

118. P. Acharya, M. Goenrich, C. H. Hagemeier, U. Demmer, J. A. Vorholt, R. K. Thauer, U. Ermler, *J. Biol. Chem.* **2005**, *280*, 13712–13719.
119. (a) W. Grabarse, M. Vaupel, J. A. Vorholt, S. Shima, R. K. Thauer, A. Wittershagen, G. Bourenkov, H. D. Bartunik, U. Ermler, *Structure* **1999**, *7*, 1257–1268. (b) V. Upadhyay, U. Demmer, E. Warkentin, J. Moll, S. Shima, U. Ermler, *Biochemistry* **2012**, *51*, 8435–8443.
120. C. H. Hagemeier, L. Chistoserdova, M. E. Lidstrom, R. K. Thauer, J. A. Vorholt, *Eur. J. Biochem.* **2000**, *267*, 3762–3769.
121. J. A. Vorholt, L. Chistoserdova, M. E. Lidstrom, R. K. Thauer, *J. Bacteriol.* **1998**, *180*, 5351–5356.
122. J. A. Vorholt, M. G. Kalyuzhnaya, C. H. Hagemeier, M. E. Lidstrom, *J. Bacteriol.* **2005**, *187*, 6069–6074.
123. U. Ermler, C. H. Hagemeier, A. Roth, U. Demmer, W. Grabarse, E. Warkentin, J. A. Vorholt, *Structure* **2002**, *10*, 1127–1137.
124. (a) M. Jormakka, B. Byrne, S. Iwata, *Curr. Opin. Struct. Biol.* **2003**, *13*, 418–423. (b) J. J. Moura, C. D. Brondino, J. Trincão, M. J. Romão, *J. Biol. Inorg. Chem.* **2004**, *9*, 791–799. (c) R. G. Efremov, L. A. Sazanov, *Biochim. Biophys. Acta.* **2012**, *1817*, 1785–1795.
125. C. S. Mota, M. G. Rivas, C. D. Brondino, I. Moura, J. J. Moura, P. J. González, N. M. Cerqueira, *J. Biol. Inorg. Chem.* **2011**, *16*, 1255–1268.
126. J. A. Vorholt, R. K. Thauer, *Met. Ions Biol. Syst.* **2002**, *39*, 571–619.
127. B. K. Pomper, O. Saurel, A. Milon, J. A. Vorholt, *FEBS Lett.* **2002**, *523*, 133–137.
128. B. K. Pomper, J. A. Vorholt, *Eur. J. Biochem.* **2001**, *268*, 4769–4775.
129. (a) U. Ermler, M. Merckel, R. K. Thauer, S. Shima, *Structure* **1997**, *5*, 635–646. (b) P. Acharya, E. Warkentin, U. Ermler, R. K. Thauer, S. Shima, *J. Mol. Biol.* **2006**, *357*, 870–879.
130. J. A. Vorholt, M. Vaupel, R. K. Thauer, *Mol. Microbiol.* **1997**, *23*, 1033–1042.
131. (a) A. Hochheimer, D. Linder, R. K. Thauer, R. Hedderich, *Eur. J. Biochem.* **1996**, *242*, 156–162. (b) A. Hochheimer, R. A. Schmitz, R. K. Thauer, R. Hedderich, *Eur. J. Biochem.* **1995**, *234*, 910–920.
132. (a) V. N. Gladyshev, J. C. Boyington, S. V. Khangulov, D. A. Grahame, T. C. Stadtman, P. D. Sun, *J. Biol. Chem.* **1996**, *271*, 8095–8100. (b) J. C. Boyington, V. N. Gladyshev, S. V. Khangulov, T. C. Stadtman, P. D. Sun, *Science* **1997**, *275*, 1305–1308.
133. H. Raaijmakers, S. Macieira, J. M. Dias, S. Teixeira, S. Bursakov, R. Huber, J. J. Moura, I. Moura, M. J. Romão, *Structure* **2002**, *10*, 1261–1272.
134. (a) R. G. Efremov, R. Baradaran, L. A. Sazanov, *Nature* **2010**, *465*, 441–445. (b) R. G. Efremov, L. A. Sazanov, *Curr. Opin. Struct. Biol.* **2011**, *21*, 532–540.
135. G. J. Crowther, G. Kosály, M. E. Lidstrom, *J. Bacteriol.* **2008**, *190*, 5057–5062.
136. (a) R. K. Thauer, K. Jungermann, K. Decker, *Bacteriol. Rev.* 1**977**, *41*, 100–180.

137. (b) http://nshs-science.net/chemistry/common/pdf/R-standard_enthalpy_of_formation.pdf (c) http://www.nist.gov/data/PDFfiles/jpcrd6.pdf (d) http://fizyczna.chem.pg.gda.pl/files/2012/10/chf_epm_cr_00.pdf
138. *The Metal-Driven Biogeochemistry of Gaseous Compounds in the Environment*, Eds P.M.H. Kroneck, M.E. Sosa Torres; Vol. 14 of *Metal Ions in Life Sciences*, Eds A. Sigel, H. Sigel, R.K.O. Sigel; Springer Science+Business Media, Dordrecht, The Netherlands, 2014.